1971

Mechanical properties of low carbon martensite

Allen L. Affolter

Department:

MECHANICAL PROPERTIES OF LOW CARBON MARTENSITE

BY

ALLEN L. AFFOLTER

A THESIS

Presented to the Faculty of the Graduate School of the

UNIVERSITY OF MISSOURI-ROLLA

In Partial Fulfillment of the Requirements for the Degree

MASTER OF SCIENCE IN METALLURGICAL ENGINEERING

1971

Approved by

David Mays (Advisor) Fred Kusslinger

Peter J. Hansen

ABSTRACT

Steels of three different compositions were heat treated and tensile tested in order to determine their mechanical properties after heat treatment. All samples had near 0.20 per cent carbon and two manganese levels -- 0.90 per cent and 1.35 per cent. One group containing the higher manganese level also had small additions of columbium and vanadium. The specimens were too brittle in the as-quenched condition to be loaded to full strength. Maximum strength and ductility were found after short time tempering at low tempering temperatures -- 2 to 15 minutes at 200° to 300°F. Higher strengths were found at the low tempering temperatures in the higher manganese steels due to the lowering of the M_s by increased manganese. The columbium and vanadium additions resulted in higher strengths due to their grain refinement effect.

ACKNOWLEDGEMENT

The author is grateful to Prof. R. V. Wolf and Dr. Fred Kisslinger for their advice and assistance given throughout the investigations and in the preparation of this thesis. The assistance and cooperation of the other members of the faculty of the Department of Metallurgical Engineering is gratefully acknowledged.

The author also wishes to express his gratitude to Inland Steel Company for providing and preparing the tensile specimens. The author is especially grateful to Mr. Logan Mair and Mr. Raymond Bello of the Quality Control Department of Inland Steel Company.

The author also wishes to express his gratitude to Mr. Raymond Fournelle for all of his assistance in the area of equipment.

TABLE OF CONTENTS

Page

LIST OF FIGURES

Figures Page

Figures

LIST OF TABLES

I. Introduction

A study aimed at investigating the mechanical properties of low carbon martensites was undertaken. The steels investigated were all near 0.20% carbon and consisted of three groups - one containing manganese of approximately 0.90%, one containing manganese of approximately 1.35%, and one containing manganese of approximately 1.35% plus small amounts of columbium and vanadium.

An important source of high strength in steels is the martensitic transformation. Martensite is usually thought of as a brittle structure. This limits its use since some ductility is usually required. However, several studies have shown that low carbon martensites can show favorable combinations of strength and ductility.

The steels studied in this work were investigated primarily in order to determine the effects of the above differences in chemical composition on the mechanical properties of the low carbon martensite.

II. Literature Review

A. Formation of Martensite

The martensitic transformation does not require diffusion and the chemical composition of the martensitic product is the same as that of the parent phase. The atoms move cooperatively, each atom shifting only slightly relative to its neighbors, so that there are always certain crystallographic orientation relationships between the martensite and the parent phase. Some atoms must change neighbors, however, since slip of one part of the crystal may be produced by the motion of the interface. "Martensite is defined in terms of how it forms, not in terms of its structure or properties. In general, martensites are not necessarily hard and strong. Even in the case of steel, the martensitic transformation does not result in high strength if the carbon content is low."[1]

A martensitic transformation is made possible by an interface which couples the lattice of the parent phase to that of the martensite with some degree of coherency. As the interface sweeps along, the parent phase is converted to martensite. This process, then, does not require thermally activated atom-by-atom jumps across the moving interface. Once nucleation occurs, martensite grows very rapidly until the interface loses its mobile character or until a barrier is reached. A barrier may be a grain boundary or a previously formed martensite plate. Further transformation must then

depend on additional nucleation and growth of smaller and smaller plates in the intervening space between the existing plates of martensite.[1]

The following quote is from "Theory of Transformations in Metals and Alloys" by J. W. Christian. "Kurdjumov concluded that nucleation rather than growth is the rate limiting step in isothermal transformation, and metallographic observations confirm that individual plates form very rapidly as in athermal martensite. Conclusive evidence that the difference in kinetic behaviour is not attributable to the growth mechanism is provided by the work of Bunshah and Mehl (1953) on the velocity of formation of individual plates in an iron-nickel-carbon alloy."[2]

The macroscopic displacements involved in martensitic transformations can generate lattice defects and distortions in the remaining parent phase which eventually become inherited by the martensitic plates. The fine-scale shear process required to form martensite may take place by either slip or twinning. In low carbon steels, slip predominates resulting in a high dislocation density. Twinning increases as the carbon level increases. If the carbon level is low enough, no internal twinning is observed.[3]

B. Martensitic Structure in Steels

In face-centered cubic austenite, the carbon atoms occupy interstitial positions at the midpoints of cube edges and the cube center. These are equivalent positions

and the carbon is equidistant from each iron atom. The distortion of austenite by carbon is, therefore, symmetrical.

In the body-centered cubic structure of iron, the carbon atoms occupy interstitial positions at the midpoints of cube edges and in the centers of the square faces. In these positions, the carbon atoms are closer to two of the iron atoms than the other four (since carbon has six nearest neighbors). The carbon atom interacts more strongly with the two nearest iron atoms than the other four and pushes them apart. This changes the lattice from body-centered cubic to body-centered tetragonal. This localized shape change is often referred to as a "distortion dipole".[1]

Another important aspect of the body-centered tetragonal lattice is that the c axis or [001] direction of the unit cell lying parallel to the dipole axis is aligned with the c axis of all other body-centered tetragonal unit cells in the martensitic crystal. If the carbon atoms were to locate themselves indiscriminately among the three sets of interstitial positions, the axes of the distortion dipoles in any crystal of martensite would be equally distributed among the three principal directions, and x-ray diffraction would reveal an expanded body-centered cubic rather than a body-centered tetragonal lattice. "...this configuration of the carbon atoms appears to be more stable than a random distribution among the three sets. Internal friction measurements disclose no tendancy for the carbon

atoms to jump from one set to another, as can be done in iron-carbon ferrites."[1]

Lattice strains are generated by the martensitic transformation. These microstrains can actually be relaxed when the individual martensitic plates are released from their surroundings by electrolytic extraction.[1] These strains are not to be confused with those due to the "distortion dipole" or the macrostrains set up by thermal gradients during the quenching of massive specimens.

C. Strength of Martensite

A number of investigators[3,4,5] have discussed the following factors which seem likely to contribute to the strength of martensite-grain size, elements in substitutional solid solution, precipitation or segregation of carbon, and the substructure of the martensite (dislocations and internal twins).

1. Grain Size

The increase in strength due to a decrease in the martensite grain size is given by a Petch type relationship, $\sigma = \sigma_o + k\ell^{-1/2}$, where ℓ is the grain diameter, k and σ_o are constants for a material in a given condition.[6] At very small grain sizes this increase in strength has been shown to be very significant.[7] However, in the range of grain sizes obtainable in conventional heat treating practice, grain size does not have a significant effect on strength.[3,8] The martensitic grain size is determined to a

first approximation by the prior austenitic grain size, since a martensite plate or needle can never be larger than the austenite grain within which it forms.[3] The constant k in the Petch type relationship is such that a decrease in prior austenite grain size from 1 mm to 10μm would raise the yield stress of the corresponding martensite by approximately 30 tons/in^2. By extrapolating this relationship to $\ell^{-1/2} = 0$, a value for the yield strength of a hypothetical single crystal of martensite is obtained; this value is roughly 25 tons/in^2.[1] In conventional practice the austenite grain size is in the region of 50μm. This corresponds to a yield strength of approximately 50 tons/in^2. The total contribution due to grain size is therefore 25 tons/in^2. If it is assumed that the addition of carbon to martensite alters the σ_o term but not the constant k in the Petch type relationship (an assumption that is valid in the case of ferrites), it can be concluded that the grain size contribution to the yield stress of high carbon martensites is relatively small.[3] However its importance could become substantial in low carbon martensites.

The work of R. A. Grange[7] indicated that the strengthening over the usual range of austenite grain sizes produced in conventional heat treating procedures (ASTM 5 to 10) is but a small fraction of what might be achieved if ultrafine grains of ASTM 15 or smaller could be developed. One method of developing the small grain sizes involves heating at the lowest temperature for complete austenitiza-

tion and severely deforming. The time between deformation and quenching is adjusted to allow the deformed austenite to recrystallize completely but to prevent appreciable grain growth. Another method involves repetitive austenitizing treatments, each of a very short duration, at a temperature barely sufficient to austenitize. The effect of prior austenite grain size on the strength of martensite tempered at 800°, 1000° and 1200°F indicate that yield strength is consistently directly proportional to $\ell_\gamma^{-1/2}$. Other effects of the ultrafine-grain size are a lowering of the M_s (for an 8640 steel) and probably a considerable loss in hardenability for carbon or very low alloy steels.[7]

R. A. Grange[7] determined the constant k in the Petch type relationship to be 3000 for the yield strength. This value applies to martensite tempered up to about 400°F. At higher tempering temperatures, the value of the constant decreases. The tensile strength was found to increase linearly with $\ell_\gamma^{-1/2}$ but the constant k was about half that of the yield strength. Ductility as measured by elongation in the tensile tests of martensite tempered at 400°F did not change significantly with the different austenitic grain sizes.

Pietikäinen[9] carried out tension tests with aged and unaged bars quenched from different austenitizing temperatures. The bars had different average largest martensite plate sizes L. He showed that the true fracture stress is linearly dependent on $L^{-1/2}$. The highest values of true

fracture stress were obtained with unaged martensite. This work also showed the relatively high ductility of unaged martensite.

Wallbridge and Parr[10] found that short austenitizing soak times of about 0.5 second offer an improvement in strength and ductility in quenched low carbon steel sheet. Relatively high soaking temperatures offer a greater improvement in strengths than lower soaking temperatures in the austenitic range. The yield strength increases less, proportionately, than the ultimate tensile strength. Probably, the increase in tensile strength simply reflects the increase in ductility that was found. That is, the increased ductility allows the steel to deform plastically further beyond the yield stress thereby delaying the initiation of fracture. The reason for the improved ductility is not evident. The increase in strength is presumably related to the refinement of the prior austenitic grain size.

2. Elements in substitutional solid solution

Irvine, Pickering, and Garstone[11] note that alloying elements generally lower the martensite start temperature and, thereby, decrease the amount of autotempering obtained during the quench. This makes it difficult to determine solid solution hardening effects of the alloying elements.

Speich and Warlimont[12] concluded that the solid solution hardening effect of nickel in carbon-free martensite accounts for about one-third of the strength of Fe-20Ni martensite. This is about one-half of the contribution expected from the

solid solution hardening effect of nickel in defect-free ferrite.

Winchell and Cohen[5] report that compression tests showed that the flow stress at 0.006 plastic strain changes by no more than about 10,000 psi between 10 and 30 weight per cent Ni in Fe-Ni martensites.

Nehrenberg et al[13] determined that chromium had no significant effect on the attainable hardness of martensite. Nor did Mn, Si, Ni or Mo which were each varied over rather wide ranges. The hardness variations were attributed to carbon and nitrogen. This is at variance with Bain[14] who reported increasing hardness with increasing chromium in Fe-0.02% C-Cr alloys. However, since the nitrogen content of the alloys studied by Bain was not indicated, it is possible that the effect he observed might be attributable to nitrogen which tends to increase with increasing chromium rather than to the actual chromium variation.

Kelly and Nutting[3] conclude that the effect of substitional solid solution is too small to be important. It is assumed that the effect of substitional elements is independent of carbon (at least for the non-carbide formers). In martensites containing strong carbide formers and appreciable amounts of carbon, the solute elements may cluster to form zones similar to those found in aluminum alloys. This clustering would give rise to chemical hardening, but large increases in yield stress would not be expected.

Busby, Hawkes and Paxton[15] report that the amount or type of alloying elements studied (principally Ni, Cr, Mo and V) - other than carbon - appeared to have essentially no effect on ductility as measured in a tensile test.

3. Carbon (or Nitrogen) in Interstitial Solid Solution

Hardness and strength of unaged martensite depend markedly on the carbon content and the carbon-strengthening does not require the prior migration of carbon atoms. Cohen[1] concludes that carbon atoms in unaged martensite must strengthen either through a tightening of the lattice bonds or through the unusual distortions existing around the carbon atoms.

Winchell's[5] work suggests that the lattice stiffness of martensite (Young's modulus) decreases with increasing nickel content and there is a further decrease with increasing carbon content. So the lattice of martensite is less stiff that that of ferrite and this offers no obvious explanation for the strength of martensite. "In addition, Krizkaja has shown by integrated-intensity x-ray measurements that the dynamic displacements of the iron atoms due to thermal vibrations in the martensite lattice become larger (atomic bonds became looser) as the carbon concentration is increased."[1] This suggests that solid solution hardening is the primary cause of martensite strengthening and that the potent effect of carbon in martensite is due to the severe dipole distortions which interact strongly with dislocations. These dislocations will bend to assume a minimum energy configura-

tion relative to the carbon atoms. In order for a dislocation in this equilibrium configuration to move under an applied stress, an extra stress is needed to raise the dislocation out of its potential trough. Beyond 0.4 weight per cent carbon, the further strengthening of martensite by carbon in solution is very small, probably indicating that the carbon atoms then lie so close together that the dipole stress fields begin to interact causing a reduction in each. Also, when the carbon atoms lie very close together, the dislocations will not be able to bend on a sufficiently small scale and more carbon atoms will then lie within the dislocation core leading to a type of interaction which has not been evaluated.

Several theories have been developed to account quantitatively for this solid solution hardening. Some of these theories have been proposed by Cracknell and Petch[16], Schoeck and Seeger[17], Fleischer[18], and Winchell and Cohen[5]. Although all of these theories are similar, they differ in their predictions. The theories of Cracknell and Petch and Schoeck and Seeger predict a linear variation of flow stress with carbon content. Fleischer predicts that the strength will depend on the square root of the carbon content. Winchell and Cohen developed a model specifically for the case of martensite which predicts that the flow stress should increase with the cube root of the carbon content. Experimental results obtained by Winchell and Cohen support this prediction up to 0.4 weight per cent carbon, but Owen et al[19] later

showed that these results would also fit a variation of flow stress with the square root of the carbon content. More recent data by Roberts and Owen[20] are consistent with this square root dependence and are, therefore, in agreement with the predictions of Fleischer.

Winchell and Cohen[5] designed a series of Fe-Ni-C alloys so that the M_s for all of the alloys was about -35°C. In this way the strength of the unaged martensite could be determined free from the problem of auto tempering. At very low carbon levels there is little difference in the strength of unaged and aged martensite but this divergence grows as carbon content is increased. They concluded that aging phenomena involving carbon diffusion can contribute materially to the strength of martensite at test temperatures above -60°C, but that the main strengthening factor is the solid solution hardening of the carbon in the martensite lattice. However, Kelly and Nutting[3] have concluded that carbon in solution is responsible for only half of the strength of high carbon martensites and that the high yield stress of plain carbon martensite must be associated to a considerable degree with some form of carbon segregation.

Nehrenberg, et al[13] found that nitrogen has a rather marked effect on the attainable hardness and this effect should not be ignored.

4. Precipitation or Segregation of Carbon

Studies of tempering kinetics have led to the conclusion

that carbon diffuses more slowly in bct martensite than in bcc ferrite. The most likely explanation for this difference is that the carbon atoms in ferrite can jump among all the octahedral interstices (3 per lattice point), while in martensite the jumping is mainly confined to those sites whose distortion dipoles contribute to the tetragonality (1 per lattice point). Calculations based on these assumptions show that the time to diffuse 10 Å will be seconds or minutes (depending on composition) at room temperature and it becomes quite small at the relatively high temperatures through which the martensite must pass after it forms during the quench.[1]

Winchell and Cohen[5] showed that diffusion dependent aging or precipitation begins at temperatures as low as -60°C and appreciable age hardening occurs above this temperature. They concluded that aging makes a contribution to the room temperature strength of martensite at all but the lowest carbon levels and that carbon diffusion in martensite is significantly more rapid than the approximate calculations had shown. This could be due to short-circuiting paths in the martensite.

Precipitation during the quench (i.e. "auto-tempering") may be extensive in steels with a high M_s temperature. Aborn[21] has identified these precipitates in low carbon steels as cementite. Ansell and Brienen[22] report that variations in the effective quenching rate gives some measure of control of the extent of this auto-tempering. In internally

twinned martensite there is little evidence of precipitation during the quench. The reason for this lack of evidence for discrete precipitate particles is probably due partly to the presence of twinning, which may mask the fine precipitates and partly to the fact that twinned martensites always have a relatively low M_s temperature.

Kelly and Nutting[3] note that, if it is assumed that the precipitation of carbon is dislocation nucleated, during the quench the dislocations will be moving and continually providing new nucleation sites as they sweep through the material. If the steel is aged after quenching, however, the dislocations will be stationary and consequently fewer sites will be available for nucleation. Since the precipitate density will be greater for precipitation during the quench, the strengthening effect of auto-tempering should be greater than that for aging after the quench.

Since the effective cooling rate affects the amount of auto-tempering, the thickness of the quenched sample may affect the precipitate distribution and size. Aborn[21], working with 1013 steel in 1/32 inch and 1/8 inch specimens, found that precipitation of extremely fine particles had occurred in some martensite plates in both samples. However, plates containing the fine particles were considerable more common in the thicker sample, which contained larger and more numerous particles. No precipitate was found near the more rapidly cooled surface of the thinner specimens. These

particles were identified as cementite by electron diffraction. He concluded that decreasing hardness and increasing alteration of the structure of low carbon martensites with increasing thickness are due to an unavoidable tempering during quenching.

5. Substructure of the Martensite
(Dislocations and Internal Twins)

When martensite forms, a macroscopic change of shape as well as an inhomogeneous shear are involved. When the inhomogeneous shear is compensated by internal twinning, the dislocation density within the martensite is not very high, but a large number of narrow twins are produced. In low carbon steels no internal twinning is observed. This implies that the inhomogeneous shear has been compensated by slip - a conclusion which is supported by the observation that the dislocation density in these low carbon martensites is high.

Internal twinning is noted with increasing frequency as the carbon content is raised. Kelly and Nutting[3] report that internal twinning is probably exhibited by no more than 1-2 per cent of the grains in a 0.1 per cent carbon steel and by about 5 per cent of the grains in a 0.2 per cent carbon steel.

Kelly and Nutting[23] proposed in 1960 that internal twinning is partly responsible for the strength of martensite. This hypothesis met with considerable opposition and a number of arguments were advanced to prove that internal twinning

has no effect on the strength of martensite. Winchell and Cohen[24] based their opposition on the fact that their linear relationship between yield strength and the cube root of the carbon content for twinned Fe-Ni-C martensites extrapolated to a value of less than 20 tons/in^2 at zero carbon. As Kelly and Nutting[3] pointed out later, if we use the relationship of yield strength varying linearly with the square root rather than the cube root of the carbon content, the yield strength at zero carbon extrapolates to a value of about 35 tons/in^2 which still indicates that the effect of internal twinning at zero carbon is small or even negligible.

Radcliffe and Schatz[25] tested the hardness of a 0.4 per cent carbon Fe-C martensite at atmospheric pressure (partially twinned substructure) and at a pressure of 42 kilobars (100% twinned substructure). The hardness increase was 180 HV (from 600 to 780 HV) which was smaller than expected leading them to conclude that the presence of fine structural twins does not make an important contribution to strength in iron-alloy martensites.

Kelly and Nutting[3] note that there is general agreement that, when the martensite structure changes from laths containing a high density of dislocations at 25 per cent nickel to internally twinned plates at 30 per cent nickel, there is no appreciable change in strength. It can be argued that, since the dislocation density in internally twinned martensites is relatively low, if the twins had no

effect on the strength the internally twinned martensite should be weaker (by some 10 to 20 tons/in^2) than lath martensite. The similarity in the strength of the two structures then leads to the conclusion that the twins provide a strengthening effect which approximately balances the loss in strength due to the decrease in dislocation density. Even if this argument is correct the effect of internal twinning on the strength of carbon-free martensites cannot be greater than 10 to 20 tons/in^2. When comparing results from twinned and untwinned martensites, it must be remembered that twinned martensite is unlikely to be 100 per cent twinned. As a result any effect due to twinning will be diluted and will never appear to its fullest extent.

Cohen[1] states that the fine structure of martensite provides a "base" for the carbon dependent strengthening in at least two ways: (a) It controls the intercept value of the experimental curve at zero carbon, and (b) it enters into the slope of carbon dependence by fixing the dislocation length.

D. Tempering of Martensite

Tempering in steels is the process of heating martensite to some temperature below the lower critical (Ac_1). It is customary to distinguish three general stages in tempering steels:

1. Precipitation of epsilon carbide

2. Transformation of retained austenite
3. Transition of epsilon carbide to cementite.

Up to about 350-400°F, epsilon carbide (hexagonal $Fe_{2.4}C$) forms at the sub-boundaries in the martensite. This causes the carbon content of the martensite to drop to about 0.25 weight per cent. The martensite remains tetragonal. The formation of the precipitate has a hardening effect which is opposed by the softening effect due to the loss of carbon from the martensite. Hardening or retarded softening may occur depending on the amount of sub-boundary carbide that precipitates.

The third stage of tempering starts about 400°F when cementite begins to precipitate concurrently with solution of the epsilon carbide. Complete solution of epsilon carbide occurs by 600°F or lower. Cementite forms as elongated films at the martensitic boundaries and as both platelets and globules within the martensite grains. Up to 700°F the boundary films coarsen, and the amount of cementite formed within the martensite grains increases.

Above 700°F the grain boundary films coarsen at the expense of the cementite formed within the acicular grains inherited from the martensite. Cementite films form at both the prior martensitic and the prior austenitic grain boundaries but appear to be more persistent at the prior austenitic grain boundaries. The cementite tends to spheroidize and to coalesce both within the grains and at the grain boundaries. Up to about 1300°, ferrite grain growth is

inhibited by the grain boundary cementite.

The above description applies to martensites in general. However low carbon martensites follow a somewhat different sequence. Due to the high M_s of low carbon steels, precipitation occurs during the quench, a process known as auto-tempering. Auto-tempering precipitates cementite and no evidence has been found for the formation of epsilon carbide during tempering of low carbon martensites.[21] With low carbon martensites, only negligible amounts of retained austenite are present so that the second stage of tempering can be ignored. As discussed in section 4, Kelly and Nutting[3] note that, if it is assumed that the precipitation of carbon is dislocation nucleated, during the quench the dislocations will be moving and continually providing new nucleation sites as they sweep through the material. This should provide a greater density of small precipitates and less grain boundary films than previously discussed for the general case of tempering. During the first stage of tempering of low carbon martensites, the precipitates grow, and the third stage follows that described for the general case.

Busby et al[15] found that in low carbon martensites (maximum carbon 0.28 per cent) essentially maximum tensile strength was obtained in the as-quenched condition and was not improved by tempering. McFarland[26] studied steels with carbon contents of 0.08 to 0.19 per cent and found no increase in yield strengths with tempering temperatures in the 400° to

600°F range. For a given tempering temperature, only minor differences were observed between steel tempered for 30 minutes and steel tempered for 2 minutes. Some evidence of 600°F embrittlement was observed for steel tempered for 30 minutes but not for steel tempered for 2 minutes.

E. Reported Mechanical Properties of Low Carbon Martensites

Wallbridge and Parr[10] investigated the effect of short soaking times in the austenite range for a 0.12 per cent carbon steel. They found strength and ductility were higher at a soaking time of 0.5 second than at longer soaking times. Elongation for a 0.5 second soak was about 4 to 4.5 per cent for all soaking temperatures and fell to values of 1.5 to 2 per cent at longer soaking times of approximately 30 seconds. The soaking temperature affected ductility only in the rate at which ductility fell off at longer times but the higher temperatures gave better ultimate strength values. The conclusion that Wallbridge and Parr reached is that the improved ductility is somehow related to the reduced prior austenite grain size and the presumed smaller martensite plate size. Expecting that the carbon in a rapidly heated, rapidly soaked steel sample would not be homogeneously distributed, they gave a pre-treatment which would encourage carbon homogeneity. The only effect was to reduce ductility as measured by tensile elongation. The conclusion reached was that it is possible that a hetero-

geneous material permits considerable slip in the low carbon regions that surround harder, higher carbon regions.

McFarland[26] investigated a series of steels with carbon contents up to 0.20 per cent which were austenitized on a commercial continuous heat-treating line and given a drastic water quench. The production heating rates were high and soaking times were short since high tonnage production makes it necessary to process the strip at high speeds. When the strip thickness was such that hardenability was not a factor, no strength differences were discerned between steels quenched from low (1650°F) and high (1900°F) austenitizing temperatures. McFarland reported that for rapid austenitization 40 to 60 per cent cold reduction was preferred. He reasoned that cold work would operate to decrease elevation of the A_3 through (1) an increase in the free energy change and (2) an increase in the carbide-ferrite interfacial area. The elongations and yield strength to tensile strength ratios were apparently insensitive to carbon content being 3 to 4.5 per cent in two inches and 0.75 to 0.79 respectively. Muir, Averbach and Cohen[27] reported 5 per cent elongation for a 0.2 per cent carbon steel in the as-quenched condition. Busby et al[15] reported on low-alloy steels of 0.14 to 0.28 per cent carbon. Using an austenitizing treatment of one hour at 1700°F, they reported good ductility and high tensile strengths in the as-quenched condition but rather low yield strength to tensile strength ratios of 0.61 to 0.68 at 0.1 per cent offset. More

specifically, they report that for a brine quench: (1) 0.16 to 0.28 per cent carbon had essentially no ductility, and (2) 0.15 per cent carbon or less had appreciable ductility in the as quenched condition. For an oil quench, they report that: (1) greater than 0.18 per cent carbon showed essentially no ductility, and (2) less than 0.18 per cent carbon showed appreciable ductility in the as-quenched condition.

Aborn[21] reports that a 43 BV 12 steel showed a 63 per cent reduction in area in the as-quenched condition at a strength level of 187,000 psi. Anderson and Fitzwilson[28] report 14 per cent elongation as-quenched for a 10 B 18 steel (c - 0.17%, Mn - 1.06%, Si - 0.27%, and B - 0.002%). The as-quenched tensile strength was about 195,000 psi and the steel was made to an austenitic fine grain melting practice.

McFarland[26] reports that the as-quenched ductility for a 0.20 per cent carbon steel was about 3.5 per cent elongation. The steel had about 2 per cent elongation after tempering for 30 minutes at 600°F and about 6.5 per cent elongation after tempering for 30 minutes at 1000°F. However no 600°F embrittlement was noticed for 2 minute tempering. The steel had 3.5 per cent elongation after tempering for 2 minutes at 600°F which is the same elongation as that shown in the as-quenched condition. After tempering for 2 minutes at 1000°F, the steel had 5 per cent elongation. No increase in yield strength was found upon tempering. McFarland reports that elongation was about 1.5 to 2 per cent following

rolling and tinning. The tinning procedure resulted in the steel being subjected to a complex series of short-time low-temperature heat treatments during the cleaning, electrolytic tinning, rinsing, tin fusion, and chemical treatment required in the process. All of the treatments except the tin fusion involve immersion in liquids up to 200°F for 1 to 2 seconds per treatment. The duration of the time in the tin fusion furnace, also 1 to 2 seconds, is sufficient to heat the tin coating to about 20°-40°F in excess of its melting point of 450°F. After tinning the yield strength to tensile strength ratio rose to about 0.97. McFarland reports that yield strength, tensile strength, and per cent elongation decreased upon tempering with a rather rapid decrease in yield and tensile strengths at about 400°F.

Busby et al[15] report that yield strength to tensile strength ratio and elongation were simultaneously improved by tempering at 212°F. The tensile strength was significantly increased probably because the better ductility leads to the avoidance of premature fracture. McFarland[26] reports that the results of his study are in general agreement with the artificial strain aging (or straining and tempering) treatments of Busby et al except that he could not duplicate the large increase in tensile elongation resulting from tempering at 212°F. However, the maximum aging time used by McFarland was only one half the 4 hours used by Busby et al to develop maximum improvement in tensile properties. Possible reasons for ductility improvement with 212°F temp-

ering are: (1) stress relief, (2) microstructural changes including carbide formation, (3) hydrogen redistribution, and (4) disordering of carbon atoms in the martensite lattice.

Aborn[21] reported that tempering at 400°F greatly increases the yield strength with a slight lowering of tensile strength and very little change in ductility. Further tempering improves the yield strength to tensile strength ratio with minor improvements in ductility. He reports the optimum tempering treatment to confer both high yield strength and high ductility to be 1 hour at about 700°F. He reports that low carbon martensites reheated to 500 to 600°F begin to show formation of cementite platelets and the mottling of the matrix (present at lower temperature tempering treatments) disappears. These two circumstances may well set the stage for decreased resistance to plastic flow and increased susceptibility to crack formation and propagation.

Muir et al[27] report a curve of elongation versus tempering temperature for a 0.20 per cent carbon steel. It shows ductility as remaining relatively constant (slight increase) up to about 700°F after which the increase is rapid. They also report that the rate of cooling from the tempering temperature (water quench or air cool) had no significant effect on the conventional tensile properties.

III. Experimental

A. Description of Samples

Plate sections were hot rolled to gauge and then normalized. The furnace atmosphere was 300 cubic feet per hour of argon and 10 cubic feet per hour of hydrogen. The plates were soaked for one-half hour at 2250°F before reduction in three passes. The temperature was between 2090° and 2235°F at the start of the first pass and was between 1335° and 1435°F at the finish of the third pass. The plate sections were taken from the one-quarter width position of larger plates and were originally 0.25" by 9" x 15". The final thickness was 0.032" to 0.038".

After hot rolling, the sheets were normalized by a one-half hour soak at 1600°F in the above mentioned controlled atmosphere. The tensile samples were then cut from the sheet and milled into 2" gauge length ASTM standard rectangular tension test specimens for sheet material from 0.005" to 0.5". The specifications for these specimens are shown in figure 2 of page 87 in the ASM Metals Handbook (1948).[29]

The chemical analyses of the samples are as follows:

Table I. Composition of Steels Studied

Steel No.	C	Mn	P	S	Si	Al	Ni	Mo	Cr	V	Cb	N
1	0.17	0.89	.011 / .012	.023 / .024	.033 / .026	.005	.01 / .02	.01	.01 / .03	.01	.002	.006 / .005
2	0.23 / 0.24	1.35	.011 / .012	.023	.033 / .036	.005	.02	.01	.03	.07	.025	.007 / .005
3	0.20 / 0.22	1.29	.011 / .012	.023	.033 / .036	.005	.02	.01	.03	.07	.025	.007 / .005
4	0.19	1.36	.013 / .014	.030 / .032	.030	.005	.01 / .03	.01	.04 / .05	.01	.002	.004 / .005
5	0.18	1.36	.013 / .014	.030 / .032	.030	.005	.01 / .03	.01	.04 / .05	.01	.002	.004 / .005
6	0.19	1.36	.013 / .014	.030 / .032	.030	.005	.01 / .03	.01	.04 / .05	.01	.002	.004 / .005

Steel number 1 was described as semi-killed, aluminum deoxidized and aluminum capped. All others were described as killed and open top. Three heats of steel are involved in the above steels, Steel number 1 being from one heat, Steels number 2 and 3 being from a second heat, and Steels number 4, 5 and 6 being from the third heat.

The tensile specimens were provided by Inland Steel Company. Reduction of the plate, milling of the specimens and chemical analyses were performed by Inland Research Laboratory and Inland Quality Control Laboratory.

The as-received normalized structures are shown in Figures 1 to 3. Figure 1 is representative of Steel number 1 which has an ASTM grain size of 7-8. Figure 2 is representative of Steels number 2 and 3 which have an ASTM grain size of 10-11. Figure 3 is representative of Steels number 4, 5 and 6 which have an ASTM grain size of 7-8.

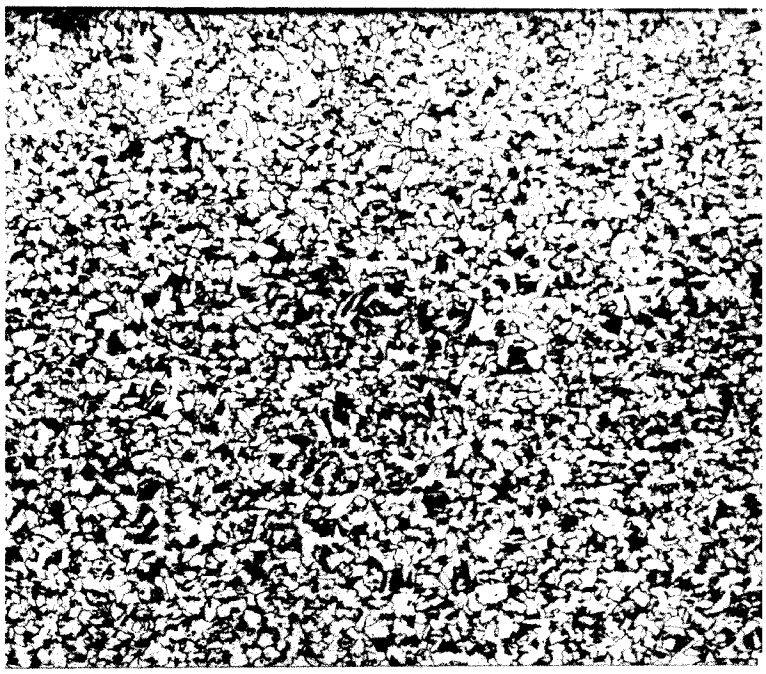

Figure 1. Steel 1. As-received normalized structure. Nital etch. 100x

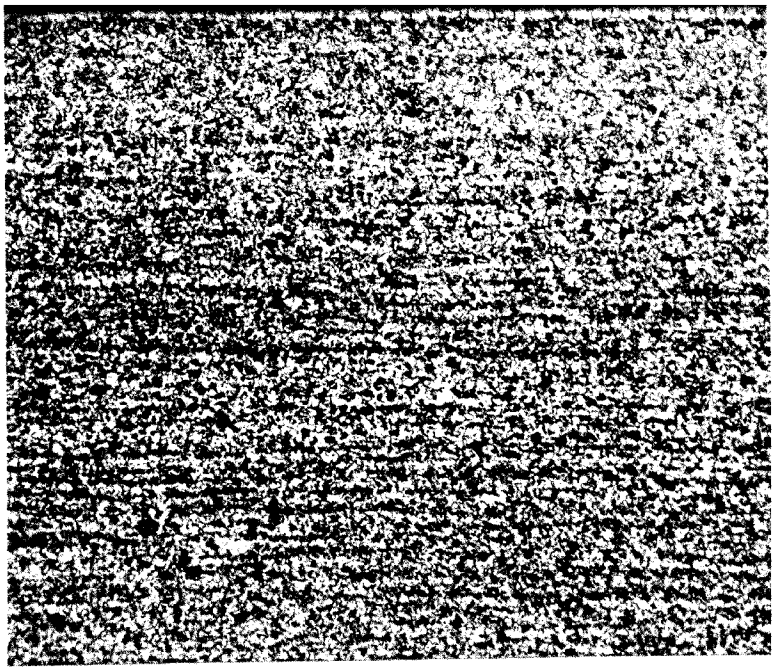

Figure 2. Steel 2. As-received normalized structure. Nital etch. 100x

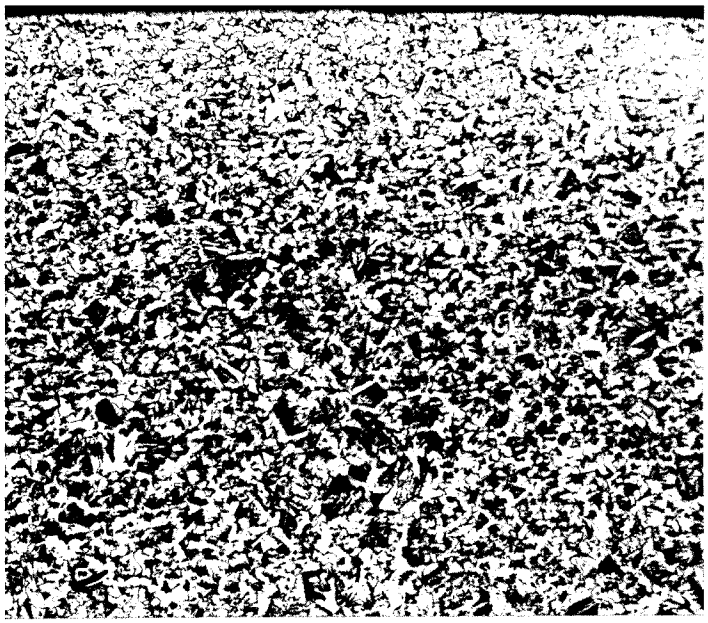

Figure 3. Steel 4. As-received normalized structure. Nital etch. 100x

B. Heat Treating Equipment

Each tensile specimen was austenitized individually by immersion in a commercial neutral salt having a working range of 1150° to 1700°F. The pot which contained the molten salt was 9.5 inches deep by 2 inches diameter. The pot was heated in a vertical, resistance heated furnace with a Gardsman (West Instrument Corporation) controller. The temperature gradient within the bath was determined at 1600° and 1650°F and was found to be no more than ± 4°F within the center 6 inches of the bath which corresponds to the necked down region of the sample. The bath temperature was checked before each austenitizing treatment by a chromel-alumel thermocouple in a stainless steel thermocouple well.

Each tensile specimen was quenched individually in a well-agitated water bath. Tempering at 200°, 300°, and 400°F was conducted in a General Electric oil tempering bath with a Bristol controller. Bath temperature varied about 5°F with position in the bath and the controller kept the temperature at any position within a range of 5°-8°F. Tempering at 500° to 800°F was conducted in a commercial neutral salt having a working range of 550° to 1100°F. The bath was a well stirred, resistance heated unit, power to which was controlled by a saturable core reactor with a Honeywell recorder-controller. This system controlled the bath temperature to ± 1/2°C.

C. Mechanical Testing

After heat treatment, hardness measurements were taken on the sample in the portion gripped by the jaws during testing. Hardness was taken on the Rockwell C scale (Brale penetrator, 150-kg load), but because the samples were relatively thin, hardness measurements were also taken on the Rockwell D scale (Brale penetrator, 100-kg load) to insure that the "anvil" did not affect the results.

Tensile specimens were tested with a floor model TT-D-L Instron tensile tester. The grips used were 20,000 pound capacity Templin grips with an expanding device to "set" the grips and prevent slippage. The Instron tester had a GR type load cell with 20,000 pounds maximum capacity, and the specimens were pulled on the 5,000 pound range to give full chart response at 5,000 pounds. The crosshead speed used was 0.10 inch per minute. Strain was measured with an Instron G-51-14 type strain gauge extensometer with a 2 inch gauge length. The servo-chart mechanism was on range 2 which gave 1 inch of chart equal to 1 per cent elongation.

Both uniform and local or necking elongation were measured. Strain between the elastic strain and that point where the load first began to drop was considered to be uniform strain. Strain between the point where the load first began to drop and the breaking point was considered to be local strain. Total strain was considered to be the sum of the uniform and local strains. Elastic strain was considered as the strain after initiation of the

load to the 0.2 per cent yield strength. The 0.2 per cent yield strength was found by constructing a line parallel to the initial straight line portion of the load-strain diagram at an offset of 0.2 per cent and noting its intersection with the load-strain diagram.

Per cent elongation was calculated by the following formula:

$$\% \text{ Elongation} = \frac{L_f - L_o}{L_o} \times 100$$

L_f represents the final length of a portion of the specimen, and L_o represents the original length of the same portion of the sample. Since the extensometer had a 2 inch gauge length, per cent elongation was 1/2 of the strain determined from the extensometer times 100.

Elongation was also determined by scribing marks 2 inches apart on the specimen and fitting the broken ends together after testing. The distance between scribe marks was taken with a beam trammel and compared to a metal scale having 0.01 inch divisions.

Ultimate tensile strength was determined by dividing the maximum load by the original cross-sectional area.

All as-quenched samples were tested the same day except as specifically noted. All samples were tempered the same day as they were quenched although tensile testing may not have taken place until as much as several days later. It was assumed that little aging occurred after tempering, so all samples should show relatively constant and small aging.

The as-received specimens showed some decarburization and some of the samples developed rust spots between the time they were received and the time they were tested. In order to avoid stress concentrators and to have all specimens tested with the same surface condition, all samples were ground lightly on a 320 grit belt grinder. In order to accurately determine the cross sectional area at the break, thickness and width surveys were run on the specimens before testing but after heat treatment.

D. Sample Identification

The specimens were identified by the code given in Table II.

Table II. Sample Identification Code

1st Digit	2nd Digit	3rd Digit
Steel number as given in Table I	Austenitizing Temperature J = 1600°F K = 1650°F S = 1700°F	Time at Austenitizing Temperature V = 1 minute Z = 3 minutes

As an example, 4KZ represents a specimen of Steel number 4 austenitized at 1650°F for 3 minutes.

E. Data

Table III. As-Quenched Mechanical Properties

Sample Code	0.2% YS(psi)	Ultimate TS(psi)	YS/TS Ratio	Extensometer Elong. (%)		Broken End Fit Elong. (%)
				Uniform	Local	
1JV	161,000	202,000	.80	0.80	0.0	*
1JZ	156,000	208,000	0.75	2.70	0.0	4.5
1KV	168,000	209,000	0.80	1.50	0.0	2.0
	169,000	221,000	0.76	2.60	0.0	*
1KZ	145,000	202,000	0.72	1.40	0.0	3.0
	162,000	193,000	0.84	0.55	0.0	*
1SV	166,000	218,000	0.76	2.00	0.0	*
	167,000	205,000	0.81	0.65	0.0	*
1SZ	161,000	215,000	0.75	1.65	0.0	3.0
3JV	161,000	202,000	0.81	0.35	0.0	*
3JZ	167,000	207,000	0.81	0.45	0.0	2.0
3KV	177,000	219,000	0.81	0.60	0.0	*
3KZ	169,000	187,000	0.90	0.20	0.0	*

Table III. (Cont.) As-Quenched Mechanical Properties

Sample Code	0.2% YS(psi)	Ultimate TS(psi)	YS/TS Ratio	Extensometer Elong. (%)		Broken End Fit Elong. (%)
				Uniform	Local	
3SV	161,000	221,000	0.73	1.00	0.0	2.0
3SZ	173,000	215,000	0.80	0.70	0.0	*
4JV	153,000	205,000	0.75	1.00	0.0	2.0
4JZ	164,000	209,000	0.78	0.90	0.0	*
4KV	166,000	194,000	0.86	0.35	0.0	0.75
4KZ	172,000	177,000	0.97	0.10	0.0	1.25
4SV	150,000	201,000	0.75	0.75	0.0	*
4SZ	155,000	202,000	0.77	0.85	0.0	*
5JV	153,000	204,000	0.75	1.10	0.0	2.25
5JZ	163,000	215,000	0.76	1.00	0.0	3.0
5KV	168,000	216,000	0.78	1.50	0.0	2.5
5KZ	185,000	190,000	0.98	0.10	0.0	*
5SV	163,000	213,000	0.77	1.25	0.0	2.5
5SZ	165,000	198,000	0.83	0.45	0.0	2.5

Table III. (Cont.) As-Quenched Mechanical Properties

Sample Code	0.2% YS(psi)	Ultimate TS(psi)	YS/TS Ratio	Extensometer Elong. (%)		Broken End Fit Elong. (%)
				Uniform	Local	
6JV	172,000	185,000	0.93	0.15	0.0	*
6JZ	149,000	209,000	0.71	1.10	0.0	*
6KV	176,000	194,000	0.91	0.25	0.0	*
6KZ	166,000	208,000	0.80	0.85	0.0	*
6SV	170,000	224,000	0.76	2.70	0.0	*
6SZ	164,000	217,000	0.76	1.45	0.0	3.0**

* Broke outside marks

** Tested more than 24 hours after quenching

Local elongation for all of the above samples is shown as zero since none was measured. Local elongation could only be measured in those samples which broke between the extensometer gauge clamps and over one-half of the samples broke outside the extensometer gauge clamps. However those samples which broke inside the gauge clamps did not show measurable local elongation. These samples typically had a fracture which was perpendicular to the tensile axis as shown by the sample on the left side in Figure 22. However it can be seen from Figure 22 that a small portion of the fracture surface failed in a ductile manner as the fracture in this portion makes a 45° angle with the tensile axis. Presumable this small area had local elongation since the broken ends did not fit together well and elongation determined by the broken and fit did not agree with that determined by the extensometer.

Representative photomicrographs of the above samples are shown in Figures 4 through 21.

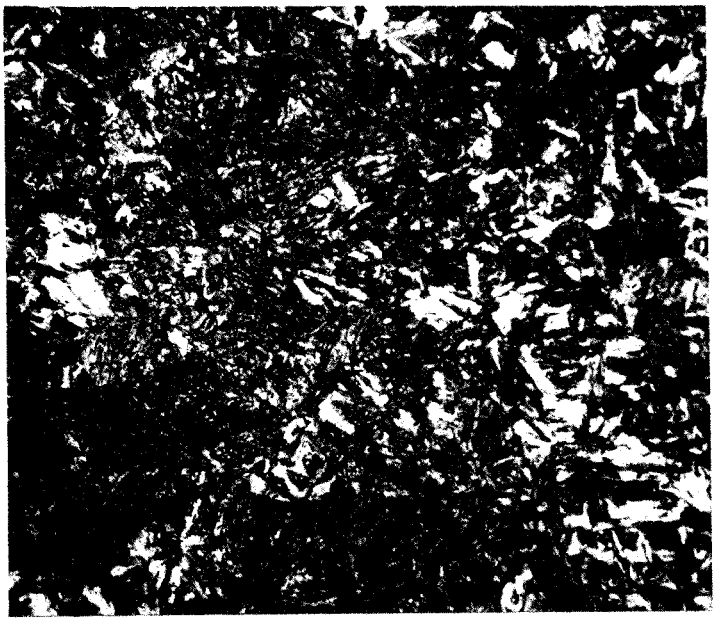

Figure 4. Sample 1JV. As-quenched structure. Austenitized at 1600°F for 1 minute. Nital etch. 500x

Figure 5. Sample 1JZ. As-quenched structure. Austenitized at 1600°F for 3 minutes. Nital etch. 500x

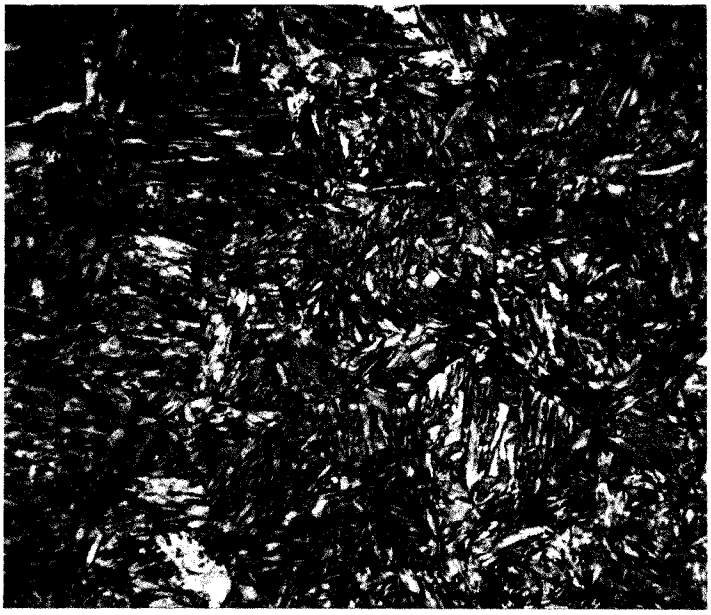

Figure 6. Sample 1KV. As-quenched structure. Austenitized at 1650°F for 1 minute. Nital etch. 500x

Figure 7. Sample 1KZ. As-quenched structure. Austenitized at 1650°F for 3 minutes. Nital etch. 500x

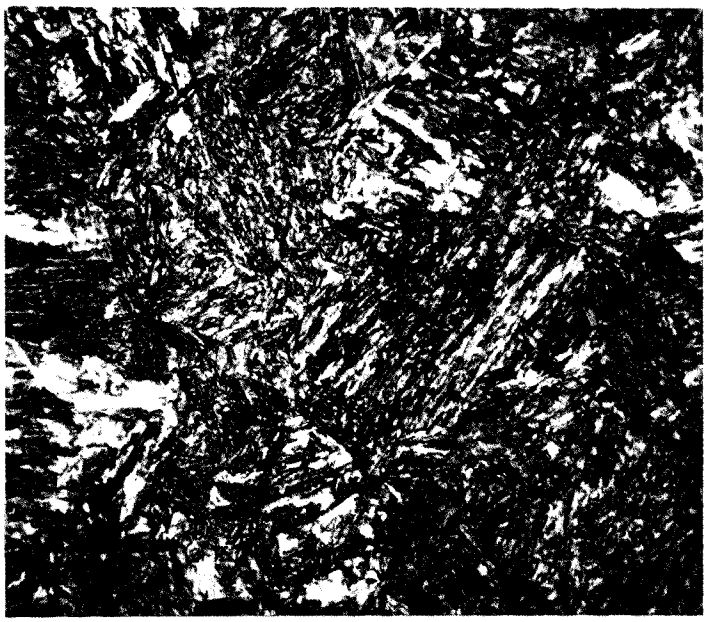

Figure 8. Sample 1SV. As-quenched structure Austenitized at 1700°F for 1 minute. Nital etch. 500x

Figure 9. Sample 1SZ. As-quenched structure. Austenitized at 1700°F for 3 minutes. Nital etch. 500x

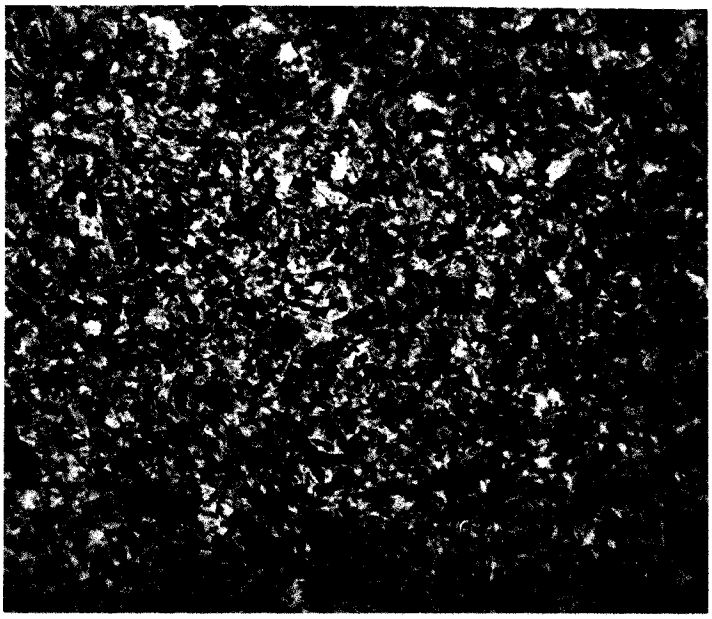

Figure 10. Sample 3JV. As-quenched structure. Austenitized at 1600°F for 1 minute. Nital etch. 500x

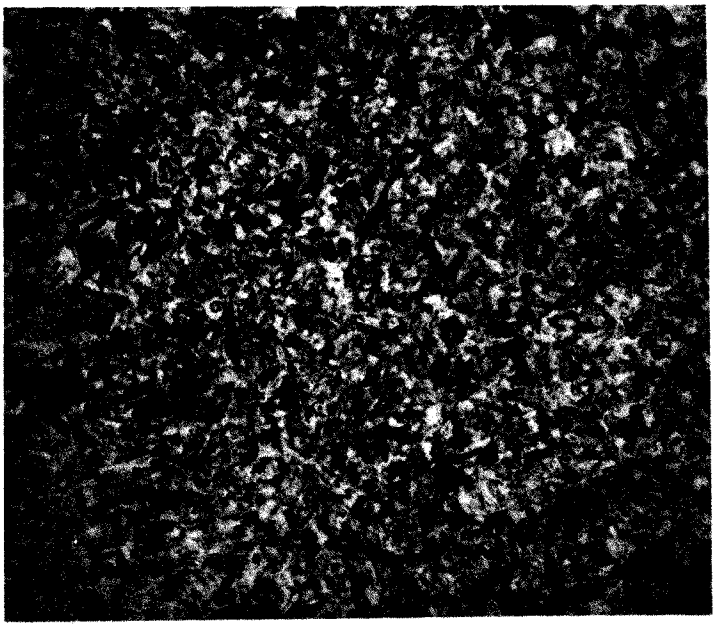

Figure 11. Sample 3JZ. As-quenched structure. Austenitized at 1600°F for 3 minutes. Nital etch. 500x

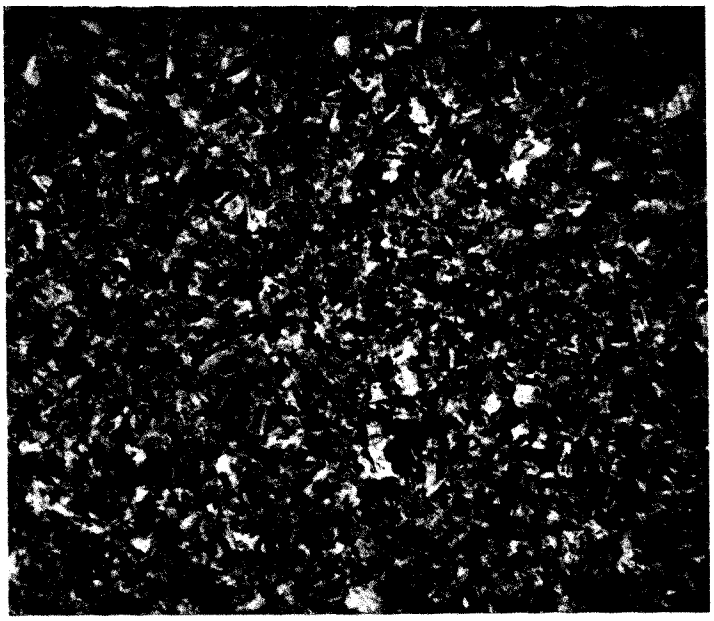

Figure 12. Sample 3KV. As-quenched structure. Austenitized at 1650°F for 1 minute. Nital etch. 500x

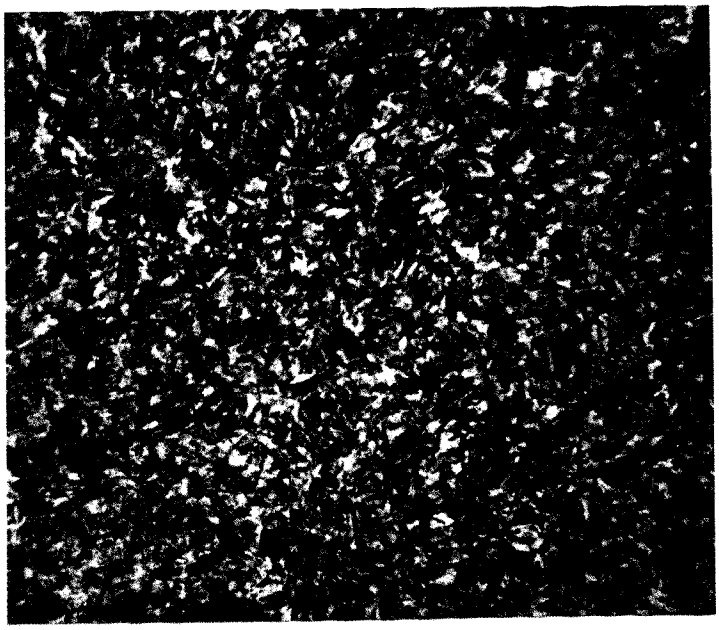

Figure 13. Sample 3KZ. As-quenched structure. Austenitized at 1650°F for 3 minutes. Nital etch. 500x

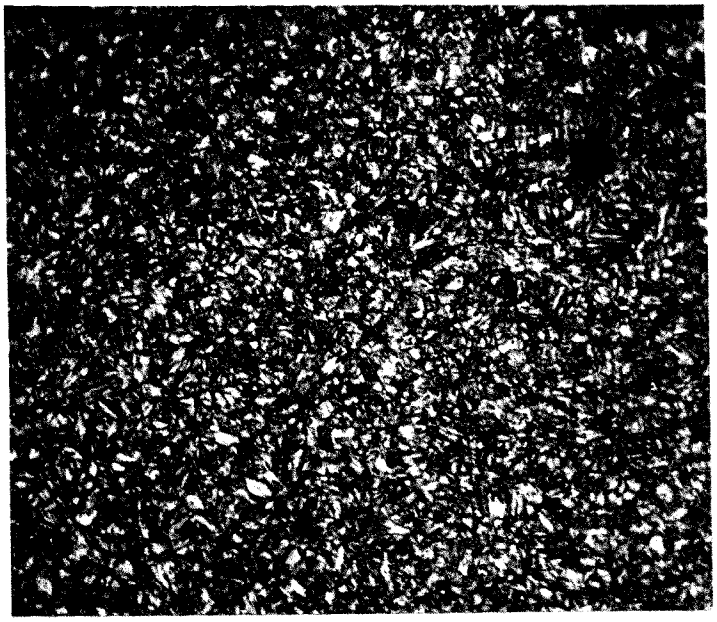

Figure 14. Sample 3SV. As-quenched structure. Austenitized at 1700°F for 1 minute. Nital etch. 500x

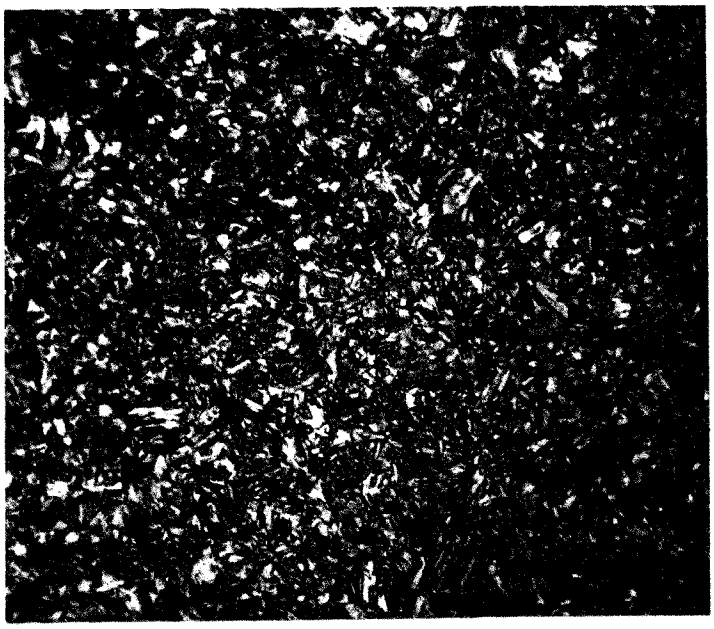

Figure 15. Sample 3SZ. As-quenched structure. Austenitized at 1700°F for 3 minutes. Nital etch. 500x

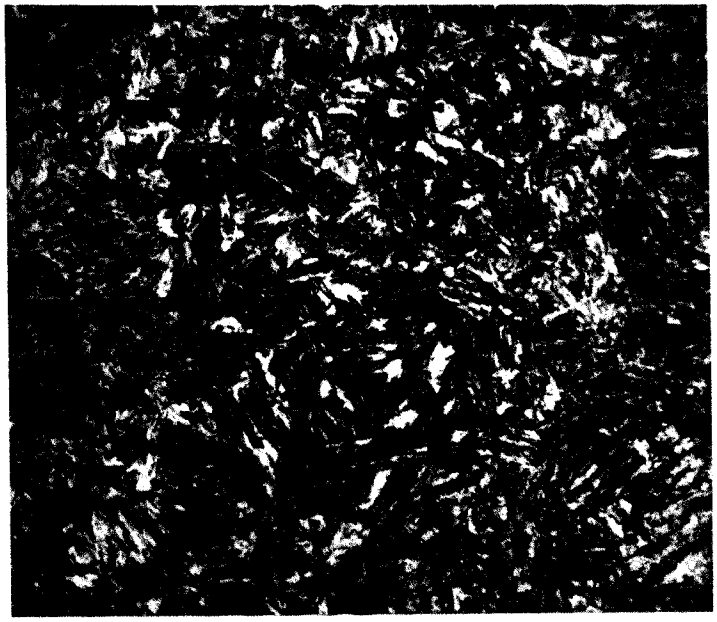

Figure 16. Sample 6JV. As-quenched structure. Austenitized at 1600°F for 1 minute. Nital etch. 500x

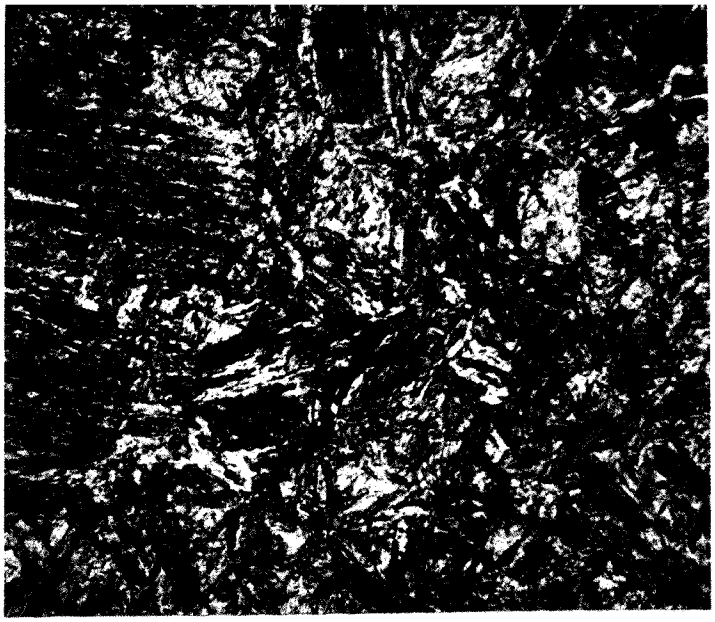

Figure 17. Sample 6JZ. As-quenched structure. Austenitized at 1600°F for 3 minutes. Nital etch. 500x

Figure 18. Sample 6KV. As-quenched structure. Austenitized at 1650°F for 1 minute. Nital etch. 500x

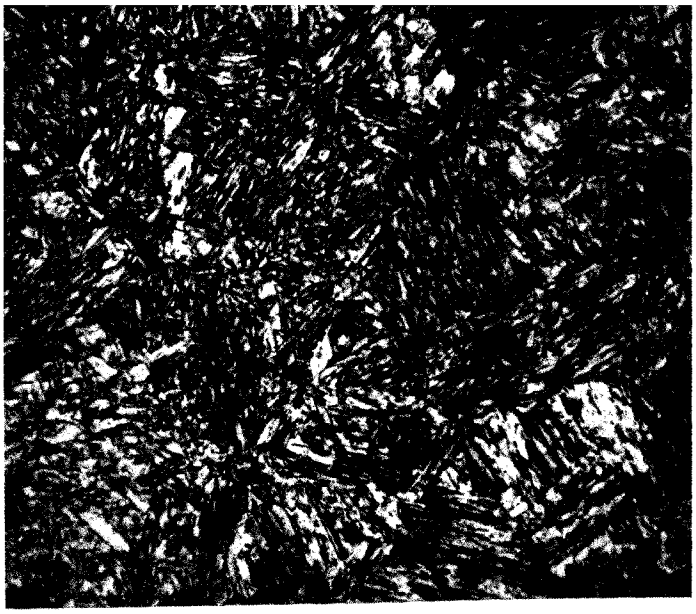

Figure 19. Sample 6KZ. As-quenched structure. Austenitized at 1650°F for 3 minutes. Nital etch. 500x

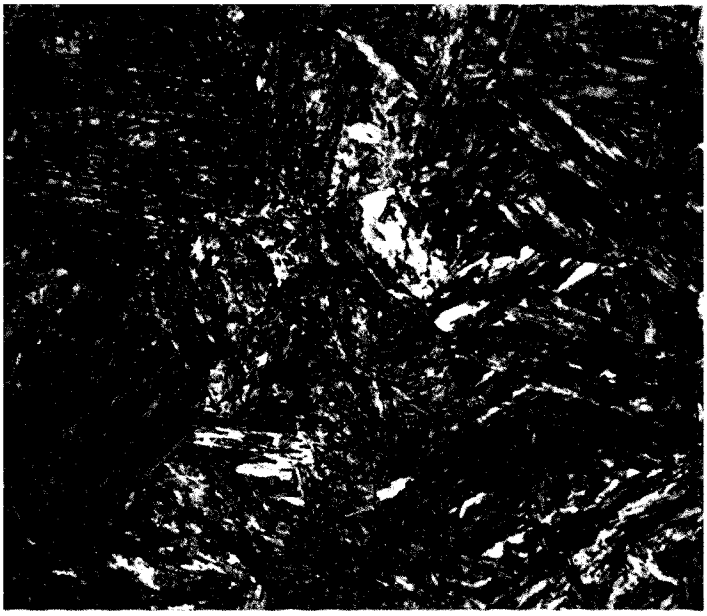

Figure 20. Sample 6SV. As-quenched structure. Austenitized at 1700°F for 1 minute. Nital etch. 500x

Figure 21. Sample 6SZ. As-quenched structure. Austenitized at 1700°F for 3 minutes. Nital etch. 500x

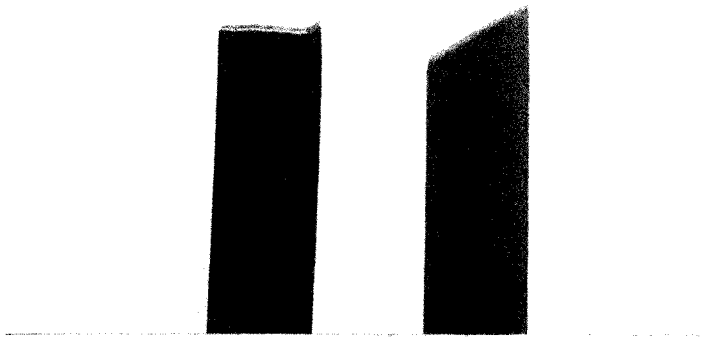

Figure 22. Representative fractures. Specimen on the left is typical for as-quenched condition. Specimen on the right is typical of tempered condition.

The prior austenite grain size was estimated by measuring the largest martensite lath lengths. Since a martensite lath can never be longer than the prior austenite grain diameter, it was assumed that the largest laths present in the microstructure would approach the prior austenite grain diameters. The ten largest laths were measured at a magnification of 500x and converted to actual size. Their average was then compared to Table 5-1, page 123, of "Mechanical Metallurgy" by Dieter[30] for determination of equivalent ASTM grain size. The results are given in Table IV below.

Table IV. Grain Sizes of As-Quenched Samples

Steel no. 1	1JV	1JZ	1KV	1KZ	1SV	1SZ
Grain Size	10	9-10	9	8	9	8-9
Steel no. 3	3JV	3JZ	3KV	3KZ	3SV	3SZ
Grain Size	11	11-12	11	11	11	10
Steel no. 4	4JV	4JZ	4KV	4KZ	4SV	4SZ
Grain Size	8-9	8-9	8	8-9	8	8
Steel no. 5	5JV	5JZ	5KV	5KZ	5SV	5SZ
Grain Size	9	8	8-9	8-9	8	8
Steel no. 6	6JV	6JZ	6KV	6KZ	6SV	6SZ
Grain Size	10	8-9	8	8-9	8	7-8

An austenitizing treatment of 1 minute at 1700°F was selected for tempering studies. The results of 2 minutes and 15 minutes at various tempering temperatures are given in Table V. The tempering temperature and time are appended to and made part of the Sample Code number.

Table V. Mechanical Properties After Tempering

Sample Code	0.2% YS(psi)	Ultimate TS(psi)	YS/TS Ratio	Extensometer Elong. (%)			Broken End Fit Elong. (%)
				Uniform	Local	Total	
1SV-200°-2	164,000	217,000	0.75	4.05	1.35	5.40	5.5
1SV-300°-2	174,000	223,000	0.78	3.30	1.00	4.30	5.0
1SV-400°-2	185,000	211,000	0.88	2.70	1.05	3.75	4.75
1SV-500°-2	169,000	195,000	0.87	2.35	1.30	3.65	4.0
1SV-600°-2	163,000	178,000	0.91	2.00	0.95	2.95	3.0
1SV-700°-2	148,000	161,000	0.92	1.60	1.25	2.85	3.0
1SV-800°-2	145,000	152,000	0.95	2.45	1.20	3.65	3.5
1SV-200°-15	183,000	227,000	0.81	2.35	0.05*	2.40	*
1SV-300°-15	168,000	215,000	0.78	3.35	0.95	4.30	5.0
1SV-400°-15	160,000	199,000	0.80	2.20	1.10	3.30	3.75
1SV-500°-15	161,000	188,000	0.86	2.85	1.20	4.05	4.5
1SV-600°-15	159,000	171,000	0.93	1.80	1.25	3.05	*
1SV-700°-15	148,000	157,000	0.94	2.90	1.30	4.20	4.0
1SV-800°-15	136,000	142,000	0.96	3.10	1.50	4.60	*

Table V (Cont.). Mechanical Properties After Tempering

Sample Code	0.2% YS(psi)	Ultimate TS(psi)	YS/TS Ratio	Extensometer Elong. (%)			Broken End Fit Elong. (%)
				Uniform	Local	Total	
2SV-200°-15	208,000	264,000	0.79	3.60	0.80	4.40	5.0
2SV-300°-15	208,000	256,000	0.82	3.15	1.05	4.20	4.5
2SV-400°-15	202,000	233,000	0.87	3.55	1.30	4.85	5.25
2SV-500°-15	194,000	209,000	0.93	2.25	0.00*	2.25	*
2SV-600°-15	183,000	190,000	0.96	2.30	1.00	3.30	3.75
2SV-700°-15	191,000	193,000	0.99	2.40	1.00	3.40	4.0
2SV-800°-15	164,000	164,000	1.00	1.20	1.15	2.35	3.0
3SV-200°-2	180,000	245,000	0.74	2.85	0.75	3.60	4.0
3SV-300°-2	204,000	259,000	0.79	2.70	0.35*	3.05	4.0
3SV-400°-2	191,000	226,000	0.84	2.55	1.00	3.55	3.75
3SV-500°-2	199,000	221,000	0.90	3.20	1.10	4.30	4.75
3SV-600°-2	192,000	206,000	0.94	2.60	0.90	3.50	4.5
3SV-700°-2	183,000	187,000	0.98	2.45	1.10	3.55	4.5
3SV-800°-2	177,000	177,000	1.00	2.00	1.25	3.25	3.25

Table V (Cont.). Mechanical Properties After Tempering

Sample Code	0.2% YS(psi)	Ultimate TS(psi)	YS/TS Ratio	Extensometer Elong. (%) Uniform	Local	Total	Broken End Fit Elong. (%)
3SV-200°-15	195,000	255,000	0.76	3.80	1.05	4.85	5.0
3SV-300°-15	210,000	261,000	0.80	3.25	1.00	4.25	4.5
3SV-400°-15	204,000	232,000	0.88	2.75	1.05	3.80	3.75
3SV-500°-15	194,000	210,000	0.92	2.10	0.95	3.05	3.5
3SV-600°-15	183,000	190,000	0.96	2.15	1.05	3.20	3.5
3SV-700°-15	174,000	177,000	0.99	1.75	1.10	2.85	3.0
3SV-800°-15	176,000	176,000	1.00	1.05	0.30*	1.35	2.5
4SV-200°-15	177,000	233,000	0.76	3.25	1.25	4.50	4.75
4SV-300°-15	172,000	221,000	0.78	4.00	1.10	5.10	5.25
4SV-400°-15	173,000	208,000	0.83	4.00	1.40	5.40	5.75
4SV-500°-15	162,000	190,000	0.85	2.80	1.15	3.95	4.0
4SV-600°-15	152,000	169,000	0.90	2.25	1.15	3.40	3.5
4SV-700°-15	149,000	161,000	0.93	2.20	1.20	3.40	4.0
4SV-800°-15	141,000	149,000	0.95	2.75	1.30	4.05	4.0

Table V (Cont.). Mechanical Properties After Tempering

Sample Code	0.2% YS(psi)	Ultimate TS(psi)	YS/TS Ratio	Extensometer Elong. (%) Uniform	Local	Total	Broken End Fit Elong. (%)
5SV-200°-15	169,000	227,000	0.74	3.10	0.10	3.20	4.5
5SV-300°-15	168,000	214,000	0.78	3.70	1.30	5.00	5.0
5SV-400°-15	166,000	209,000	0.79	2.60	0.95	3.55	4.0
5SV-500°-15	157,000	191,000	0.82	2.85	1.10	3.95	4.0
5SV-600°-15	155,000	175,000	0.88	2.65	1.15	3.80	4.5
5SV-700°-15	150,000	160,000	0.93	2.40	1.25	3.65	4.0
5SV-800°-15	139,000	148,000	0.94	3.30	1.45	4.75	4.75
6SV-200°-15	183,000	232,000	0.79	3.90	1.20	5.10	5.75
6SV-300°-15	168,000	210,000	0.80	3.40	1.30	4.70	5.0
6SV-400°-15	169,000	204,000	0.83	3.25	0.10*	3.35	*
6SV-500°-15	167,000	189,000	0.88	2.15	1.05	3.20	3.75
6SV-600°-15	163,000	179,000	0.91	1.95	1.00	2.95	3.0
6SV-700°-15	150,000	162,000	0.93	2.50	1.20	3.70	3.5
6SV-800°-15	136,000	145,000	0.94	2.60	0.00*	2.60	*

* Broke at gage marks

Hardness measurements were taken across the face of one grip end of the tensile specimen. In general the reported values are based on one test only. However when the measurement differed more than about 3 points (on either the R_C or R_D scale) from the other measurements on the specimen, an additional measurement was made to confirm the hardness value. The reported value is then the average of the two measurements. The edge hardness impression was made between 1/8" to 1/4" from the edge and the center hardness impression was made on the center of the face. Hardness values are reported in Tables VI and VII.

Table VI. As-Quenched Hardnesses

Sample Code	Edge			Center			Edge		
	R_D	Equiv. R_C	R_C	R_D	Equiv. R_C	R_C	R_D	Equiv. R_C	R_C
1JV	59-1/4	45-1/4	45-1/2	57.5	42-1/2	42-1/2	51.75	35	36-1/4
"	56-3/4	41-3/4	43-1/2	53-1/2	37-1/2	40-3/4	55-1/2	40-1/4	43
1JZ	53-1/2	37-1/2	39	55	39-1/2	42-1/2	54-1/2	39	42-1/2
"	56-1/2	41-1/2	44-1/2	49	31-3/4	36	57	42	45
1KV	56	40-3/4	40-1/2	54	38	36-1/2	56-3/4	41-3/4	42-1/4
"	58-1/2	44	46	51-1/4	34-1/2	37	57	42	44-1/2
1KZ	57-1/4	42-1/4	43-1/2	56	40-3/4	44	56-3/4	41-3/4	44-3/4
"	56-3/4	41-3/4	43-1/2	56	40-3/4	44	57-1/2	42-1/2	44-1/4
1SV	58-1/2	44	45-1/2	56-1/2	41-1/2	41-1/2	59	44-3/4	45-1/2
"	54-1/2	39	42-1/2	46-1/2	28-1/2	34	57	42	44
1SZ	57-1/2	42-1/2	44-3/4	56-1/4	41-1/4	43-1/2	58-1/2	44	45-1/2
"	58-1/4	43-3/4	45-3/4	55-1/2	40-1/4	43	57-1/2	42-1/2	45
3JV	58-1/2	44	45	58-1/4	43-3/4	45-1/2	59-1/4	45-1/4	47
3JZ	60-1/4	46-1/2	47-1/2	58	43-1/2	46	59-1/4	45-1/4	47-3/4
3KV	59-1/4	45-1/4	46-1/2	57	42	43-1/2	59-1/4	45-1/4	45-3/4

Table VI. (Cont.) As-Quenched Hardnesses

Sample Code	Edge			Center			Edge		
	R_D	Equiv. R_C	R_C	R_D	Equiv. R_C	R_C	R_D	Equiv. R_C	R_C
3KZ	59-1/2	45-1/2	47-3/4	59-1/4	45-1/4	48	58	43-1/2	45-1/2
3SV	61	47-1/4	48-3/4	59-1/2	45-1/2	47-1/4	58-1/2	44	47-1/4
3SZ	60-1/4	46-1/2	48-1/2	56-3/4	41-3/4	47-1/4	60-1/2	46-3/4	47-1/2
4JV	58-1/4	43-1/2	43	55-1/2	40-1/4	42-3/4	57	42	44-3/4
4JZ	58-1/2	44	45-1/2	58	43-1/2	45	57-3/4	43	44-1/4
4KV	59-1/4	45-1/4	45-3/4	58-1/2	44	43-1/2	57-3/4	43	44-1/4
4KZ	59	44-3/4	46	58-3/4	44-1/2	44-1/2	58	43-1/2	46
4SV	59-1/2	45-1/2	46-1/4	59	44-3/4	45-3/4	59	44-3/4	46
4SZ	58-1/2	44	45-1/2	58	43-1/2	45-1/2	58-1/4	43-3/4	44-1/2
5JV	56-3/4	41-3/4	44	56-3/4	41-3/4	43	57-1/4	42-1/2	44
5JZ	58-1/4	43-3/4	45-1/2	57	42	45-1/4	58	43-1/2	46
5KV	59	44-3/4	45-1/2	58	43-1/2	45	59-1/2	45-1/2	46-1/2
5KZ	58-3/4	44-1/2	45-1/2	57-3/4	43	44-1/2	58	43-1/2	44
5SV	58	43-1/2	45-1/2	54-1/4	38-1/4	42	58-1/4	43-3/4	44-1/2
5SZ	57-1/2	42-1/2	45	56-1/4	41-1/4	43-1/4	57	42	44

Table VI. (Cont.) As-Quenched Hardnesses

Sample Code	Edge			Center			Edge		
	R_D	Equiv. R_C	R_C	R_D	Equiv. R_C	R_C	R_D	Equiv. R_C	R_C
6JV	58-1/4	43-3/4	45-3/4	57	42	44-3/4	56-3/4	42	44
6JZ	56-3/4	41-3/4	44	55-1/2	40-1/4	43	55-3/4	40-1/2	42-1/2
6KV	59-1/2	45-1/2	46	56-1/4	41-1/4	43-1/2	58-1/4	43-3/4	46
6KZ	58	43-1/2	45	56	40-3/4	43-1/2	56-3/4	41-3/4	43-3/4
6SV	56	40-3/4	42-1/2	55-1/2	40-1/4	42-1/4	55-1/2	40-1/4	42
6SZ	58	43-1/2	45	57-1/2	42-1/2	43-1/2	57-1/4	42-1/2	44

Table VII. Hardnesses After Tempering

Sample Code	Edge			Center			Edge			Equiv. R_C Average
	R_D	Equiv. R_C	R_C	R_D	Equiv. R_C	R_C	R_D	Equiv. R_C	R_C	
1SV-200°-2	58-1/4	43-3/4	43-1/4	55	39-1/2	41	56	40-3/4	39-1/2	41-1/4
1SV-300°-2	56	40-3/4	42-1/4	55	39-1/2	39	57-1/2	42-1/2	44-3/4	41
1SV-400°-2	57-3/4	43	44-1/4	55-1/2	40-1/4	42-1/4	55	39-1/2	42-1/4	41
1SV-500°-2	55-1/4	40	41-3/4	52-1/2	36-1/4	39	55-1/4	40	42	38-3/4
1SV-600°-2	52-1/2	36-1/4	37-3/4	52-1/2	36-1/4	37-3/4	52	35-1/2	38-1/2	36
1SV-700°-2	52-1/4	36	36-3/4	50-3/4	34	36-1/4	51	34-1/4	36-1/4	34-3/4
1SV-800°-2	49-1/4	32	33-1/2	50-1/4	33-1/2	35	50	33	33-3/4	32-3/4
1SV-200°-15	58-1/2	44	45-1/2	56-1/4	41-1/4	42-1/2	58	43-1/2	44-1/2	43
1SV-300°-15	58	43-1/2	44-1/2	56-1/2	41-1/2	41-1/4	58	43-1/2	44-1/4	42-3/4
1SV-400°-15	57	42	43-3/4	57	42	42-3/4	57	42	43-1/2	42
1SV-500°-15	54-1/2	39	40	51-1/2	34-3/4	38-1/4	53-1/2	37-1/2	39-1/2	37
1SV-600°-15	50-1/2	33-3/4	36-1/2	46-1/2	28-1/2	30-3/4	50	33	35-3/4	31-3/4
1SV-700°-15	50	33	35	50	33	34-1/4	50	33	35-1/4	33
1SV-800°-15	48-1/2	31	31-1/2	47-3/4	30	30	48-3/4	31-1/2	31-1/2	30-3/4

Table VII (Cont.). Hardnesses After Tempering

Sample Code	Edge			Center			Edge			Equiv. R_C Average
	R_D	Equiv. R_C	R_C	R_D	Equiv. R_C	R_C	R_D	Equiv. R_C	R_C	
2SV-200°-15	61-3/4	48-1/2	49-3/4	59-3/4	45-3/4	47-1/4	60	46	47-3/4	46-3/4
2SV-300°-15	62	49	48	59-3/4	45-3/4	47-3/4	60-3/4	47	48-1/2	47-1/4
2SV-400°-15	60	46	47	59	44-3/4	45-3/4	60	46	46-1/4	45-1/2
2SV-500°-15	56	40-3/4	42-1/4	56	40-3/4	41-1/2	56	40-3/4	42-1/4	40-3/4
2SV-600°-15	55-1/2	40-1/4	41	53-1/4	37-1/4	38	55-1/4	40	40-1/2	39-1/4
2SV-700°-15	53-1/4	37-1/4	38-1/4	51	34-1/4	35-1/2	53-3/4	37-3/4	37-3/4	36-1/2
2SV-800°-15	52-1/4	36	36-1/2	52	35-1/2	36-1/4	52	35-1/2	36	35-3/4
3SV-200°-2	61-1/2	48	48-3/4	60	46	48	61-1/4	47-3/4	48-3/4	47-1/4
3SV-300°-2	60-1/4	46-1/2	47-3/4	59-1/4	45-1/4	46-3/4	59-1/2	45-1/2	47-1/2	45-3/4
3SV-400°-2	59-3/4	45-3/4	46	57-1/4	42-1/2	42-1/4	58-1/2	44	46	44
3SV-500°-2	57	42	44	57-3/4	43	44	57-3/4	43	44	42-3/4
3SV-600°-2	55	39-1/2	41-1/2	53-1/2	37-1/2	41-1/2	55	39-1/2	39-3/4	38-3/4
3SV-700°-2	53-1/2	37-1/2	39	52-1/2	36-1/4	38-1/4	54-1/2	39	38-3/4	37-1/2
3SV-800°-2	52-1/2	36-1/4	37-1/2	52-1/4	36	37-1/2	52-1/4	36	37-1/2	36

Table VII (Cont.). Hardnesses After Tempering

Sample Code	Edge			Center			Edge			Equiv. R_C Average
	R_D	Equiv. R_C	R_C	R_D	Equiv. R_C	R_C	R_D	Equiv. R_C	R_C	
3SV-200°-15	61-3/4	48-1/2	49	59-1/4	45-1/4	46-3/4	60-1/4	46-1/2	48-3/4	46-3/4
3SV-300°-15	59	44-3/4	47	59-1/2	45-1/2	47-1/2	59-3/4	45-3/4	46-1/4	45-1/4
3SV-400°-15	59-1/2	45-1/2	46-3/4	59-1/2	45-1/2	44-1/2	59-1/4	45-1/4	45-3/4	45-1/2
3SV-500°-15	56-1/4	41-1/4	40-3/4	55-1/4	40	41-1/4	56	40-3/4	42-1/4	40-3/4
3SV-600°-15	53	37	39	52-3/4	36-1/2	38-1/4	54-1/4	38-1/4	40	37-1/4
3SV-700°-15	53	37	38	52-1/2	36-1/4	38	53-1/4	37-1/4	38-1/2	36-3/4
3SV-800°-15	51-1/4	34-1/2	35-3/4	50-1/4	33-1/2	35-1/4	51-1/2	34-3/4	36	34-1/4
4SV-200°-15	59-3/4	45-3/4	46-1/2	59	44-3/4	45-1/4	58	43-1/2	45	44-3/4
4SV-300°-15	58-1/2	44	44-1/2	56-1/2	41-1/2	43-1/2	57-1/2	42-1/2	44	42-3/4
4SV-400°-15	57	42	42	56	40-3/4	41-3/4	57	42	42-1/4	41-1/2
4SV-500°-15	54-3/4	39-1/4	40-3/4	55-1/4	40	40	54-1/2	39	39-3/4	39-1/2
4SV-600°-15	53-1/2	37-1/2	38	53-1/2	37-1/2	37	52-1/4	36	36-1/2	37
4SV-700°-15	50-1/4	33-1/2	35	51	34-1/4	35	51	34-1/4	35	34
4SV-800°-15	48-3/4	31-1/2	32	48-1/4	30-3/4	31-1/4	49	31-3/4	31	31-1/4

Table VII (Cont.). Hardnesses After Tempering

Sample Code	Edge			Center			Edge			Equiv. R_C Average
	R_D	Equiv. R_C	R_C	R_D	Equiv. R_C	R_C	R_D	Equiv. R_C	R_C	
5SV-200°-15	58-1/2	44	46	57	42	43	56-3/4	41-3/4	44-3/4	42-1/2
.5SV-300°-15	57-1/2	42-1/2	43-1/2	57-1/4	42-1/2	43	59	44-3/4	44-3/4	43-1/4
5SV-400°-15	57	42	42-3/4	56	40-3/4	42	57	42	43-1/2	41-1/2
5SV-500°-15	54	38	39	53	37	39-1/4	55	39-1/2	39-3/4	38-1/4
5SV-600°-15	52-1/4	36	36-1/4	51-3/4	35	37	52-1/4	36	36-1/2	35-3/4
5SV-700°-15	50-1/2	33-3/4	34-1/2	51-1/4	34-1/2	35-1/4	50	33	34-1/2	33-3/4
5SV-800°-15	49	31-3/4	32	49	31-3/4	32	49	31-3/4	31-1/4	31-3/4
6SV-200°-15	58-1/2	44	45-1/4	57	42	43-1/4	58-3/4	44-1/2	45-3/4	43-1/2
6SV-300°-15	55-1/2	40-1/4	43	56-1/4	41-1/4	42-1/4	57-1/2	42-1/2	43-1/4	41-1/4
6SV-400°-15	57-1/2	42-1/2	42-1/2	56	40-3/4	43-1/4	57	42	43	41-3/4
6SV-500°-15	54	38	39-1/4	54-3/4	39-1/4	39-1/2	55	39-1/2	40	39
6SV-600°-15	51-3/4	35	37-1/4	52-1/2	36-1/4	37-1/4	53	37	38-1/2	36
6SV-700°-15	50-3/4	34	35-1/4	51-1/2	34-3/4	35-1/2	51	34-1/4	35-3/4	34-1/4
6SV-800°-15	48-1/2	31	32-1/2	48-1/2	31	32-1/4	49-1/4	32	33-1/4	31-1/4

Table VIII. Average As-Quenched Hardnesses

Steel No.	Equivalent R_C (from R_D)		
	Center	Edge	Avg.
Steel No. 1-as-quenched	38.0	41.75	40.5
Steel No. 3-as-quenched	43.75	45.38	44.75
Steel No. 4-as-quenched	43.5	43.88	43.75
Steel No. 5-as-quenched	41.75	43.5	43.0
Steel No. 6-as-quenched	41.0	42.38	42.0

Table IX. Variations in As-Quenched Hardnesses

Steel No.	Equivalent R_C (from R_D)		
	Max. Variation within a specimen	Average specimen Max. variation	Max. variation for the steel
Steel No. 1-as-quenched	10-1/4	5.1	16-3/4
Steel No. 3-as-quenched	5	3.0	5-1/2
Steel No. 4-as-quenched	3-1/4	1.7	5-1/4
Steel No. 5-as-quenched	5-1/2	2.1	7-1/4
Steel No. 6-as-quenched	4-1/4	2.0	5-1/4

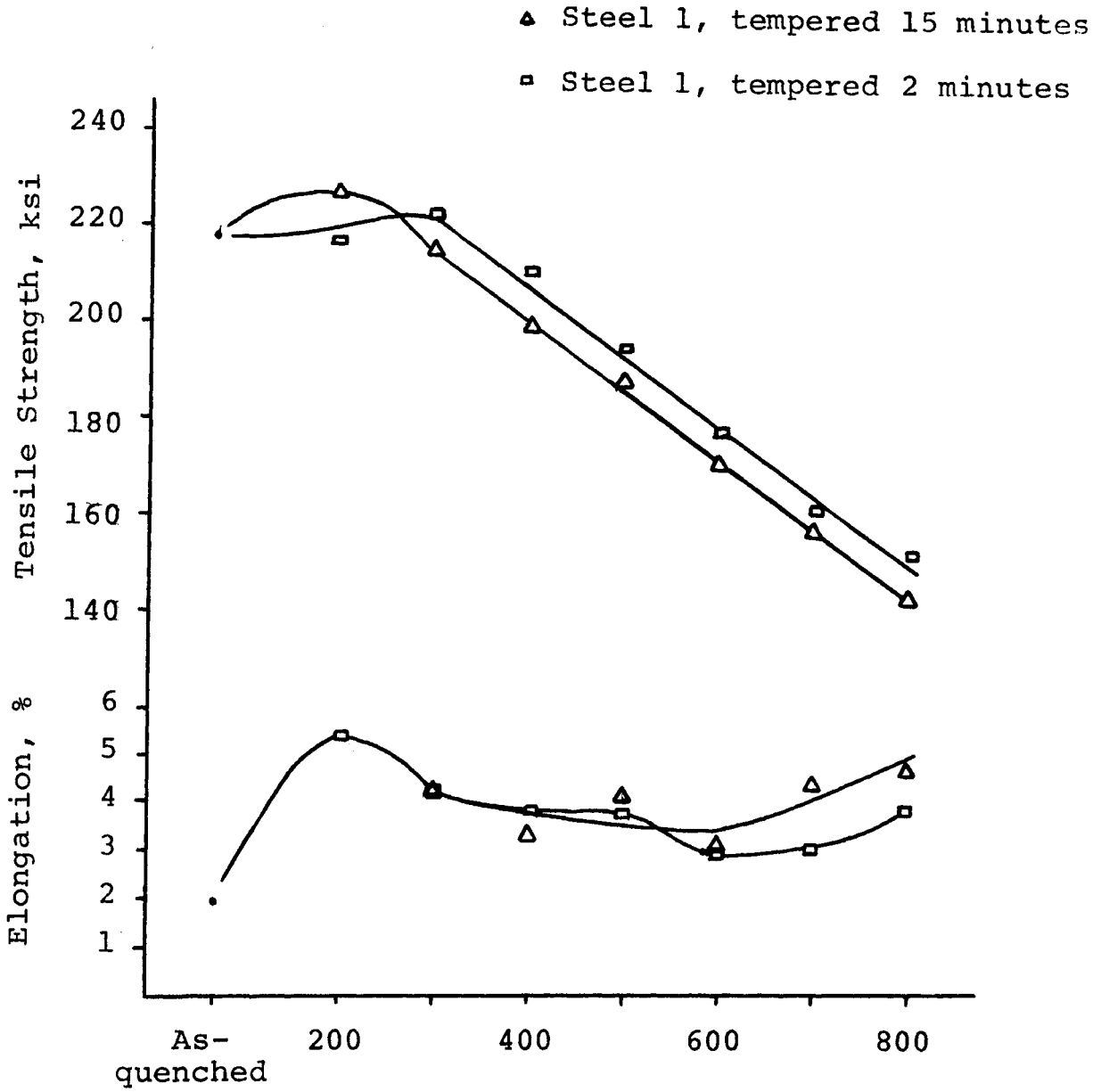

Figure 23. Tensile strength and elongation of Steel 1 after 2 minutes and 15 minutes at various tempering temperatures. All Steel 1 specimens were austenitized at 1700°F for 1 minute.

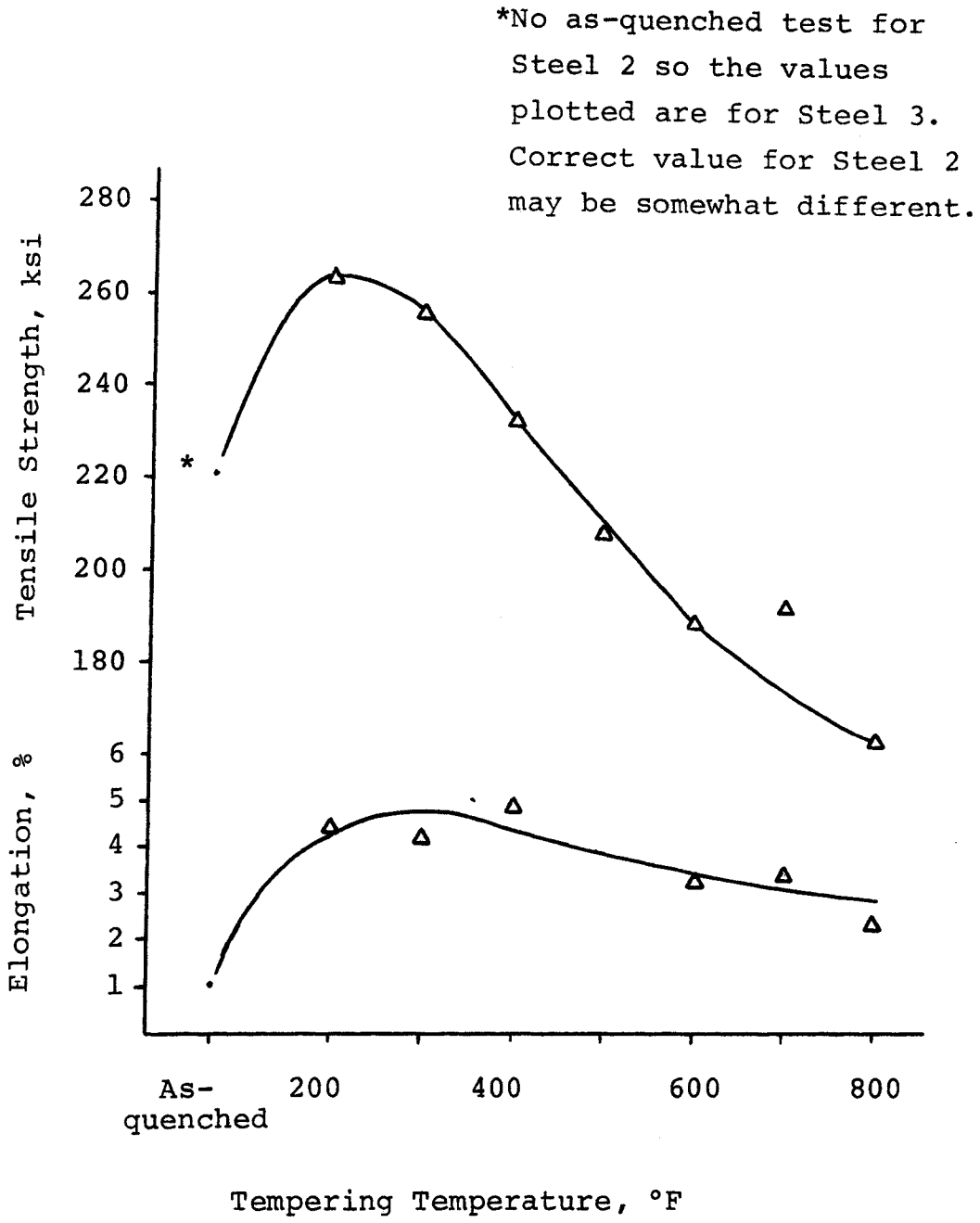

Figure 24. Tensile strength and elongation of Steel 2 after 15 minutes at various tempering temperatures. All Steel 2 specimens were austenitized at 1700°F for 1 minute.

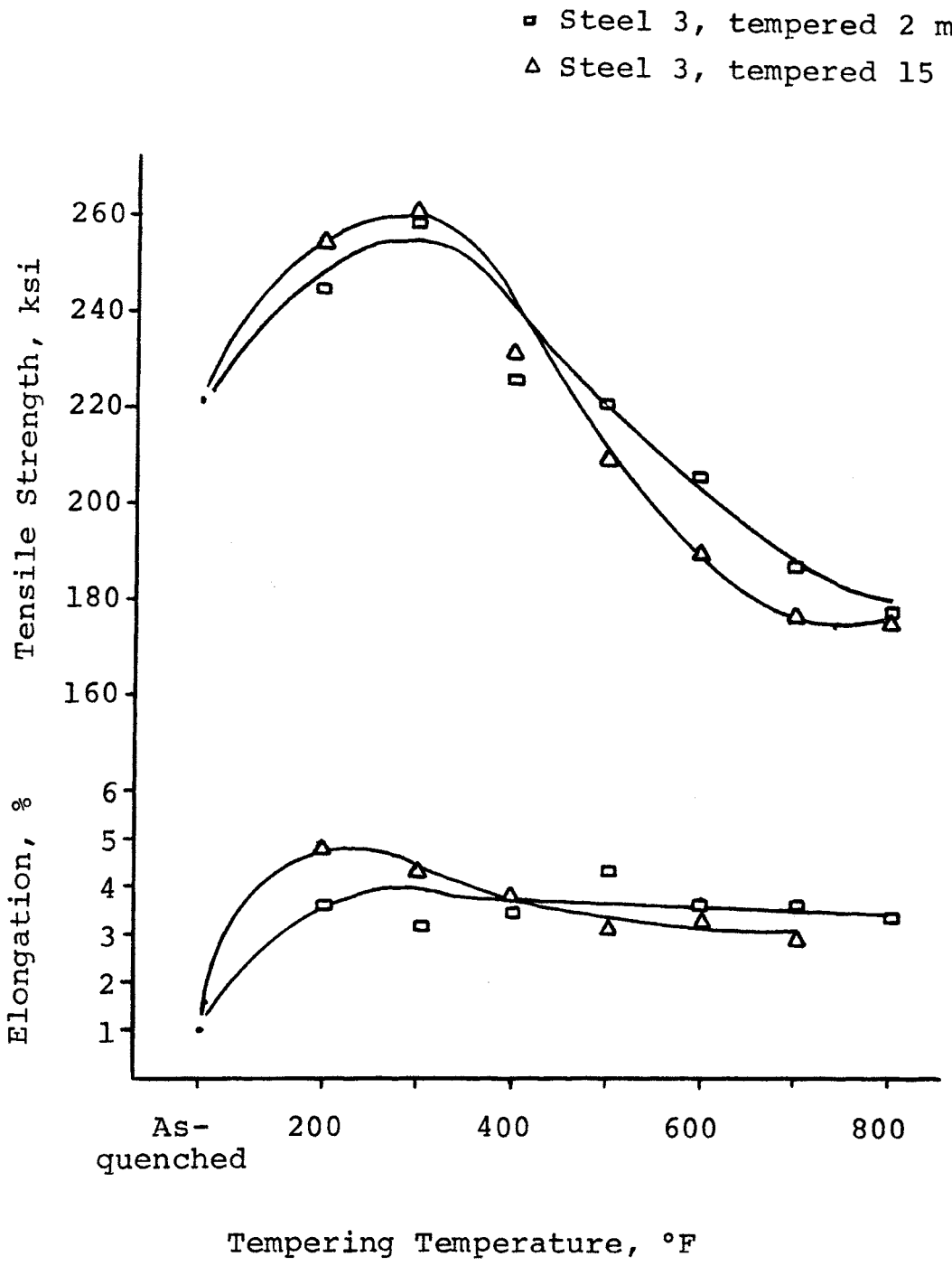

Figure 25. Tensile strength and elongation of Steel 3 after 2 minutes and 15 minutes at various tempering temperatures. All Steel 3 specimens were austenitized at 1700°F for 1 minute.

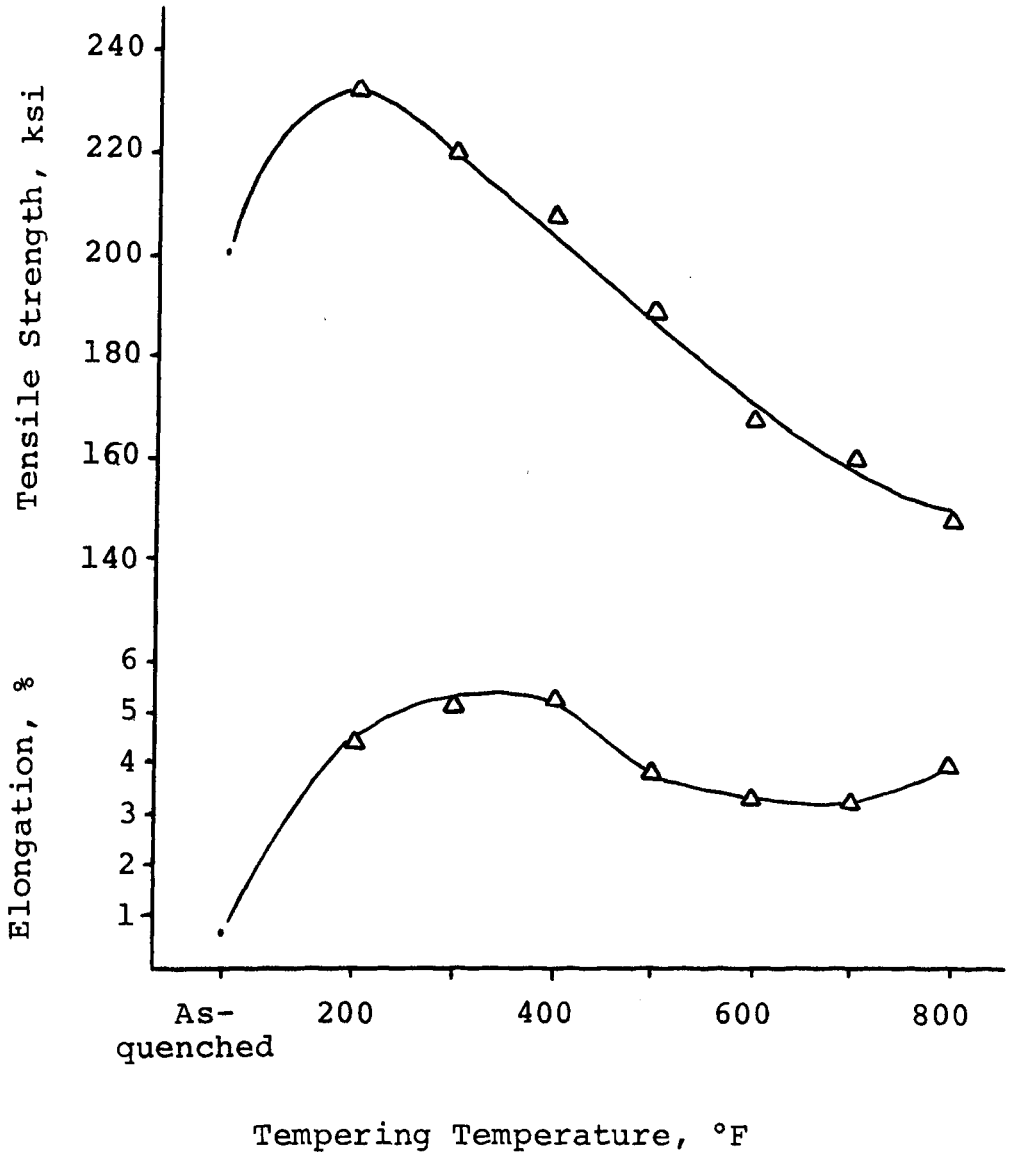

Figure 26. Tensile strength and elongation of Steel 4 after 15 minutes at various tempering temperatures. All Steel 4 specimens were austenitized at 1700°F for 1 minute.

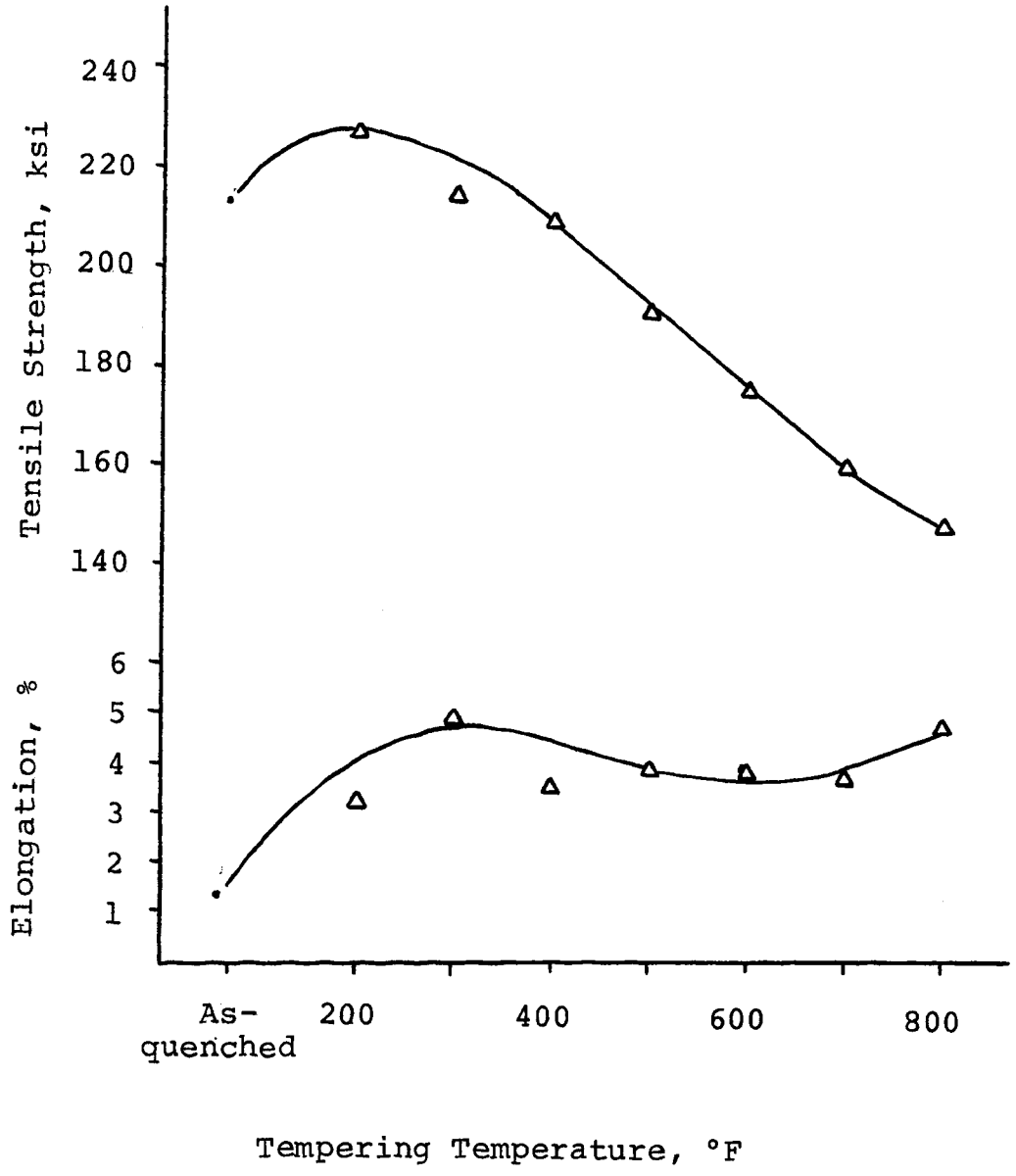

Figure 27. Tensile strength and elongation of Steel 5 after 15 minutes at various tempering temperatures. All Steel 5 specimens were austenitized at 1700°F for 1 minute.

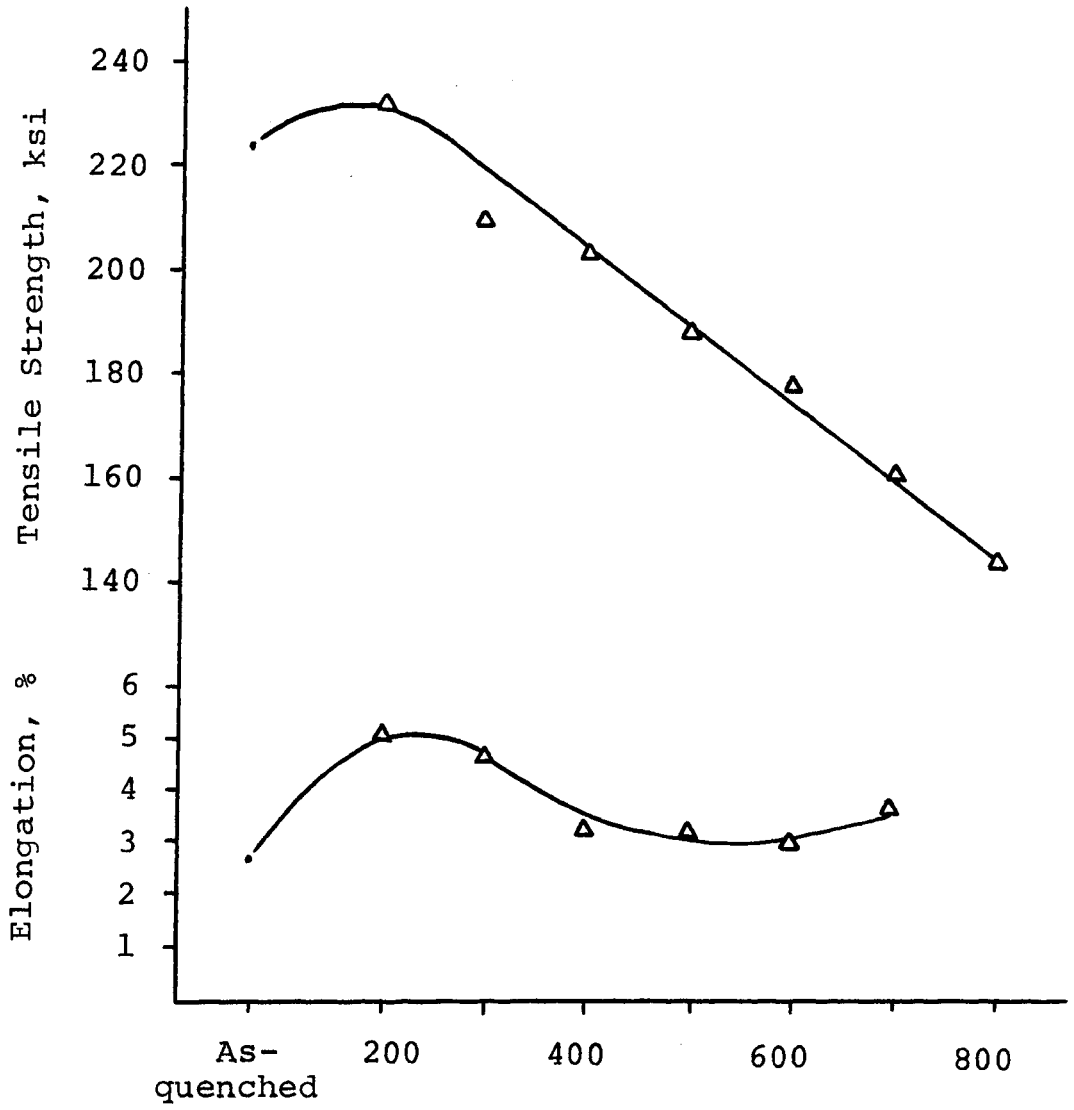

Figure 28. Tensile strength and elongation of Steel 6 after 15 minutes at various tempering temperatures. All Steel 6 specimens were austenitized at 1700°F for 1 minute.

IV. Discussion of Results

By reference to Table I, it can be seen that the samples have basically three chemical analyses -- that represented by the Steel 1, that represented by Steels 2 and 3, and that represented by Steels 4, 5 and 6.

The formula for determination of M_s given by Grange and Stewart[31] based on C, Mn, Ni, Cr, and Mo gives the following results:

Table X. Martensite Start for Steels Tested

Steel No.	Sample No.	M_s °F
1	2	825
2	4A	750
3	4B	770
4	5	777
5	5A	783
6	6A	777

The starting structures were the same for all samples of a certain steel. The molten salt gave a constant, relatively high heating rate. Therefore, the only variables affecting austenitization were austenitizing temperature and the time at austenitizing temperature. By varying the temperature and time at temperature the effect of austenitizing conditions can be studied in as-quenched samples since the quenching rate was held as constant as

possible and the M_s was a constant within a certain steel. The A_3 was determined from the iron-carbon diagram which indicated that the A_3 would range from about 1580°F for the steel 1 samples to about 1540°F for the steel 2 samples. It would appear then that an austenitizing temperature of 1600°F would be sufficient to completely austenitize all samples if the times at temperature were long enough. In order to investigate the effects of austenitizing temperatures, two other temperatures were selected -- 1650°F and 1700°F. Higher temperatures were not used since they would have exceeded the working range of the salt in the austenitizing salt bath. Since short austenitizing times cannot be avoided if high tonnage rates are to be achieved in a continuous heat treating unit, the times selected were 1 minute and 3 minutes.

The as-quenched tensile strengths did not vary in a predictable manner. The ductilities were quite low averaging about 1.5% for Steel number 1, 0.5% for Steel number 3, 0.7% for Steel number 4, 0.9% for Steel number 5, and 1.1% for Steel number 6. The low ductilities in combination with the random variation in tensile strengths seems to indicate that the samples are not being loaded to their full strength but are failing prematurely instead.

The yield to tensile strength ratio varied from 0.71 to 0.97 in a random manner. This compares to a value of 0.75 to 0.79 reported by McFarland[26] for as-quenched samples. Premature failure would result in a yield to tensile ratio

that was too high, so these results further support the assumption that the as-quenched samples are failing prematurely.

It is noted that ductilities as measured by the broken end fit do not compare well with those determined by the extensometer. As shown in Figure 22, the as-quenched samples usually had a brittle type fracture perpendicular to the tensile axis with a small amount of ductile fracture at the edge. This small amount of ductile fracture prevented the broken ends from being fitted together closely. At these relatively small elongations, any error in measurement is greatly magnified.

As-quenched hardnesses showed no effect of the various austenitizing conditions. However the photomicrographs of Figures 4 through 21 and the data in Table IV show that the 1 minute treatment at 1600°F had the smallest martensitic lath size which increased in a rather regular manner until at the 3 minutes treatment at 1700°F it was approximately equivalent to the normalized grain size. The light etching grains in the as-quenched structure were more numerous at the lower temperatures and shorter times. They are probably the results of a lack of homogenization in the prior austenite. However they were still present at 1700°F after 3 minutes austenitization. They were not uniformly distributed but were more numerous at about one quarter thickness positions. Kentron hardness testing with a Knoop identor and a 10 gram load indicated

690 KHN for the white etching grains and about 530 KHN for the matrix. No conversion chart was available for KHN's determined with such a light load. Using a chart valid for KHN's determined with a load of 500 grams or greater, the white etching grains were R_C 58 while the matrix was R_C 51. The conversion is not accurate as can be seen from Table VI which indicates that none of the samples show hardness levels that high. However, the difference in hardness may be relatively accurate and this indicates that the white etching constituent is about 7 points on the R_C scale harder. It appears that these grains then are simply slightly higher carbon martensites which were the last formed and had less opportunity to autotemper. These observations conform to those found by Busby et al.[15]

Photomicrographs were taken from near the break and from the center of the necked down portion of the sample in those cases where they did not coincide. No differences in microstructure were found.

Hardness tests were made on both the R_C scale and the R_D scale. The R_D values were then converted to equivalent R_C values. It was found that the equivalent R_C values were consistently lower than those values from the R_C scale. This indicates that the thicknesses were too small to prevent an anvil effect when using the R_C scale. Rockwell superficial hardness measurements were made on 6 as-quenched samples using a Brale indentor and a 45 Kg load.

Agreement was generally good between the superficial hardnesses converted to R_C scale and the R_D hardnesses which were converted to R_C scale. However the superficial hardness often were lower than the R_D hardnesses -- about 2 to 3 points R_C after converting to the R_C scale. Therefore, it would appear that the R_D hardnesses are also showing some anvil effect. However, no great error appears to be involved and, accordingly, only equivalent R_C hardness determined from the R_D scale will be considered in the subsequent discussion of results. All conversions from R_D scale were made from Table 38 in the Appendix of "Principles of Metallographic Laboratory Practice" by G. L. Kehl.[32]

Even though the hardness data showed no trend within a certain steel due to austenitizing conditions, the average hardnesses of one steel should be compared to that of another steel in order to determine effects of changes in chemical composition. Referring to Table VIII, it can be seen that Steel number 1 had the lowest average hardness of R_C 40.5, Steels 4, 5 and 6 had slightly greater average hardnesses of R_C 43.75, 43.0, and 42.0 respectively due to their higher carbon contents and possibly due to their lower M_S, and Steel number 3 had the highest average hardness of R_C 44.75 due to its higher carbon content. Steels 4 and 6 have essentially the same chemical analyses and therefore should show the same as-quenched hardness.

That they do not is evidence that the quench was not entirely uniform resulting in soft spots. This is also shown by the hardness variation within an as-quenched sample. For Steel number 1 the maximum variation in hardness within a sample was R_C 10-1/4 while the average of all maximum variations within a sample for this steel is R_C 5.1. Referring to Table IX, it can be seen that the hardness variation is greatest for Steel number 1, but that variations exist in all steels. It must be remembered that hardnesses were taken at one end of the sample and not on the necked down portion. In order to check the hardness variation throughout the sample, one of the Steel number 1 samples was quenched and 104 hardness tests were made covering both sides and the entire length of the sample while concentrating primarily in the necked down region. The maximum variation was 5 points on R_C scale and no systematic variations were found. It should also be noted that different samples of Steel number 1 quenched to different hardness levels. Table IX shows a range of almost 17 points on the R_C scale from the highest hardness to the lowest hardness found in Steel number 1 in the as-quenched condition. This differs greatly from the other steels which show all samples within a particular steel number as quenching to essentially the same hardness level.

It appears then that any effects of tested austenitizing conditions on the as-quenched properties are hidden by

these premature failures. However, it should be noted that McFarland[26] reported that no strength differences were discerned between steels quenched from low (1650°F) and high (1900°F) austenitizing temperatures.

The most striking result of the tempering was the large increase in per cent elongation after low temperature tempering, usually after 2 minutes at 200°F. The tensile strengths also increased after this low temperature tempering. Since both Busby et al[15] and McFarland[26] report that essentially maximum strength was achieved in the as-quenched condition, it appears that the increase is more apparent than real and results from the increased ability of the samples to be loaded to their true strength levels as a result of the improved ductilities. Another factor pointing to this explanation is that the strength increase is the greatest for those samples showing the lowest as-quenched ductilities.

Since the as-quenched samples apparently did not show their true strengths, some effects of the differences in chemical analyses of the various steels may be shown by comparing their strengths after low temperature tempering which appear to reflect their true strength levels more closely than the results of tests in the as-quenched condition. Differences in strength level should result from: (a) differences in carbon level, (b) differences in M_s due to carbon and manganese levels, (c) solid solution hardening by manganese, and (d) differences in grain size.

McFarland[26] reports that the maximum tensile strength (as-quenched condition) is given by the following formula:

$$TS = 119 + 560\ (\%C)$$

Comparing the maximum strengths as given by McFarland's formula to maximum tensile strengths found after low temperature tempering gives the following results.

Table XI. Comparison of Maximum Tensile Strengths

Steel No.	Tensile Strength (by McFarland), psi	Actual Tensile Strength After Tempering, psi
1	214,000	227,000
2	252,000	264,000
3	242,000	259,000
4	225,000	233,000
5	220,000	227,000
6	225,000	232,000

When comparing the results above, it must be noted that McFarland's formula was based only on carbon and the manganese levels were approximately 0.45%. Therefore all the tested samples had a M_s which was lower than that accounted for by McFarland. Accordingly, all samples showed higher tensile strengths than given by McFarland's formula and this can be accounted for by the lower M_s. However, McFarland predicts an increase in strength of 11,000 psi for Steels 4 and 6 over that of Steel 1 while an actual increase of only 6,000 psi and 5,000 psi respectively was

found. The tempering required to determine maximum strength could account for these differences. It appears then that the above data indicates a strengthening effect due to a depressed M_s but a smaller than predicted increase due to carbon alone, probably due to the tempering.

McFarland's formula predicts an increase in strength of 38,000 psi and 28,000 psi for Steels 2 and 3 respectively over that of Steel 1 while an actual increase of 37,000 psi and 32,000 psi respectively is found. Here, then, the effect of carbon appears to be present in the full amount predicted by McFarland. However Steels 2 and 3 have a smaller grain size than that of Steel 1 due to the additions of Cb and V. A strength increment is to be expected from this decreased grain size according to the Petch type relationship described by R. A. Grange.[7] The constant K is given as 1500 by R. A. Grange for the tensile strength of lightly tempered martensite. Accordingly, a difference of about 8,000 psi between Steel 1 and Steels 2 and 3 should be present due to the differences in grain size shown in Table IV. This would offset the loss in strength due to tempering shown by Steels 4 and 6. In addition, R. A. Grange indicated that small grain size may decrease the M_s so an additional strength increment may be gained by Steels 2 and 3. Thus, it appears that the previous conclusions regarding the effect of decreased M_s resulting from increased manganese and the lower than predicted effect of carbon, probably due to tempering, that

were reached for Steels 4 and 6 in comparison with Steel 1 are valid. In addition, the effect of grain size is shown.

The effect of solid solution hardening by manganese is not shown by the above data but it should be noted that Kelly and Nutting[3], Nehrenberg et al[13], and Busby et al[15] report that substitutional solid solution hardening does not occur or it is too small to be important.

Since Kelly and Nutting[3] have reported that the proportion of lath martensite versus twinned martensite should have no effect on the strength, the effect of depressing the M_s should be limited to the effects of auto-tempering -- that is, the proportion of carbon in solution as opposed to carbon in precipitates. In this connection, it should be noted that the low temperature tempering does not result in a hardness decrease.

The yield to tensile strength ratios of the low temperature tempered samples compares very well to those reported by McFarland[26] for as-quenched samples of 0.75 to 0.79

Comparison of the tempering curves shows that Steel 1 reaches its maximum strength at 200°F for a tempering time of 15 minutes and 300°F for a tempering time of 2 minutes. After that the strength decreases in a linear fashion up to a tempering temperature of 800°F with the 2 minute tempered samples being consistently about 8,000 psi stronger than the 15 minute tempered samples. The

per cent elongations show a somewhat different pattern with maximum elongation for the 2 minute tempered samples being reached at 200°F and the maximum elongation for the 15 minute tempered samples being reached at 300°F. The Steel 1 samples tempered for 15 minutes show considerable scatter but elongation would appear to be relatively constant between 300° and 800°F except for a low value at 600°F. The Steel 1 samples tempered for 2 minutes show relatively constant elongation at 300°, 400° and 500°F with a decrease at 600° and 700°F. All tempered samples had considerably better elongation values than the as-quenched samples.

Steel 4 also showed maximum strength at 200°F with 15 minute tempering. When compared to Steel 1 samples with 15 minutes tempering, Steel 4 samples show somewhat higher strengths at the low tempering temperatures but the curves nearly coincide at higher temperatures. Steel 1 samples showed a linear decrease while Steel 4 samples show a linear decrease up to the high tempering temperatures where the curve begins to flatten. Maximum elongation is not reached until 400°F and elongations decrease at 500°, 600° and 700°F with only a slight increase at 800°F. Again, all tempered elongations are much better than the as-quenched values.

Steels 4 and 6 should be virtually identical. The tensile curves nearly coincide and the elongations are very similar with the main differences being that Steel 6 reaches

maximum ductility at lower tempering temperatures and the decrease in elongation begins at 400° rather than 500°F.

For all practical purposes, Steel 5 is the same as Steels 4 and 6 with the only difference being that Steel 5 has a reported carbon level 1 point lower than Steels 4 and 6. Accordingly, the tensile strength curves nearly coincide. Elongations for Steel 5 show much the same trend as for Steels 4 and 6 being the greatest at 300°F and show only a slight decrease at higher temperatures.

Steels 2 and 3 have higher carbon contents than the other steels as well as additions of Cb and V. Steel 2 has a higher carbon content than Steel 3. Steel 2 samples show maximum tensile strength at 200°F while Steel 3 samples show maximum tensile strength at 300°F. From 400° to 800°F, the tensile strength curves for 15 minutes tempering for both Steel 2 and 3 nearly coincide while the tensile strength curve for 2 minutes tempering for Steel 3 is about 10,000 psi higher at the higher tempering temperatures.

The Steel 2 samples show considerable scatter in elongations but the 15 minutes tempered samples for both Steels 2 and 3 show the same general pattern as for all other steels investigated. Maximum elongation is shown at 200° to 300°F with a slight decrease at higher tempering temperatures. Steel 3 samples tempered for 2 minutes

did not show a ductility decrease until somewhat higher temperatures than the 15 minutes tempered samples. One difference in the Steels 2 and 3 samples from the other steels is that Steels 2 and 3 samples show no tendancy towards an increase in per cent elongation at 800°F while the other steels (with one exception) showed at least a small increase in elongation at 800°F.

All steels then showed the same general pattern differing only in degree. All steels showed an increase in tensile strength at low tempering temperatures and a rather rapid decrease after about 400°F. All steels showed improvement in elongation after tempering at 200° to 300°F with a slight decrease at higher temperatures. All tempered elongations were much better than the as-quenched elongations. Elongation determined by fitting the broken ends of the samples together was acceptably close to that determined by the strain gauge extensometer for the tempered samples in contrast to the poor correlation shown for the as-quenched samples. The broken ends fit together very well for the tempered samples probably due to the fact that these samples showed the same type fracture across the sample. The fractures were at a 45° angle to the tensile axis as shown by the sample on the right in Figure 22. All steels tempered at low tempering temperatures showed yield to tensile strength ratios which were similar to those reported by McFarland[26] for as-quenched samples and increased in a regular manner with increased

tempering temperatures. The only differences in yield to tensile strength ratio improvement were the starting ratios and the maximum ratios reached at the highest tempering temperatures.

The improvement in elongation values after tempering at 200° to 300°F is in agreement with the data reported by Busby et al[15]. Irvine et al[11] reported that, for a 0.20 per cent carbon steel, the as-quenched structure contained many carbide particles and the first effect of tempering was to increase this precipitation. Starting at about 400° and extending to about 600°F, the precipitates coarsened and films of carbide formed around the martensite plate boundaries. This temperature range coincides with the temperature range at which elongations began to decrease for the steels reported in the present investigation.

One effect of Cb and V, which are carbide formers, should be to retard the tempering process and this is apparently why Steels 2 and 3 showed no tendancy toward ductility improvement at 800°F. At some temperature greater than 800°F, the carbide films would be expected to break up by spheroidization and improvement in ductility would result.

McFarland[26] reports as-quenched ductility for 0.18 to 0.20 per cent carbon and 0.45 per cent manganese steels to be about 4 per cent. Steel number 1 is comparable to McFarland's steels except for the manganese content which

is approximately doubled to 0.90 per cent. As-quenched Steel 1 samples show about 1.5 per cent elongation as compared to about 4 per cent elongation for McFarland's steels. Steels 4, 5 and 6 are comparable to McFarland's steels except for the manganese content which is approximately tripled to 1.35 per cent. As-quenched Steels 4, 5 and 6 samples show about 1 per cent elongation as compared to about 4 per cent elongation for McFarland's steels. However all the higher manganese samples showed the same favorable combinations of strength and ductility as those reported by McFarland after short time tempering at low temperatures - 2 to 15 minutes at 200° to 300°F.

V. Conclusions

A. The as-quenched ductilities for all steels were too low for the samples to be loaded to full strength in the tensile test. Steels of these chemical analyses could probably not be used commercially in the as-quenched condition.

B. Simultaneous improvement in both tensile strength and ductility is displayed by all samples after low temperature (200° to 300°F) tempering.

C. The yield to tensile strength ratio increases continuously with increasing tempering temperatures up to values of 0.94 to 1.00 at 800°F.

D. Some decrease in ductility is found at tempering temperatures of 500° to 700°F but the ductilities at these temperatures are still high in comparison to the as-quenched ductilities.

BIBLIOGRAPHY

1. Cohen, M. (1962) "The Strengthening of Steel". Trans. Met. Soc. of AIME, Vol. 224, p. 638-656.

2. Christian, J. W. (1965) "Theory of Transformations in Metals and Alloys". Pergamon Press, p. 813.

3. Kelly, P. M. and Nutting, J. (1965) "Strengthening Mechanisms in Martensite". ISI Spec. Rpt. 93, p. 166-170.

4. Chilton, J. M. and Kelly, P. M. (1968) "The Strength of Ferrous Martensite". Acta Metallurgica, Vol. 16, p. 637-656.

5. Winchell, P. G. and Cohen, M. (1962) "The Strength of Martensite". Trans. ASM, Vol. 55, p. 347-361.

6. Petch, N. J. (1953) "The Cleavage Strength of Polycrystals", JISI, Vol. 174, p. 25-28.

7. Grange, R. A. (1966) "Strengthening Steel by Austenite Grain Refinement". Trans. ASM, Vol. 59, p. 26-48.

8. Cohen, M. (1963) "On the Development of High Strength in Steel", JISI, Vol. 201, p. 833-841.

9. Pietikäinen, J. (1968) "Effect of Plate Size, Aging, and Test Temperature on the Fracture of Martensite in Iron-Nickel-Silicon-Carbon Steels". JISI, Vol. 206, p. 834-839.

10. Wallbridge, J. M. and Parr, J. G. (1967) "Effect of Rapid Heat Treating on Mechanical Properties of Low-Carbon Steel Sheet". JISI, Vol. 205, p. 750-755.

11. Irvine, K. J., Pickering, F. B. and Garstone, J. (1960) "The Effect of Composition on the Structure and Properties of Martensite". JISI, Vol. 196, p. 66-81.

12. Speich, G. R. and Warlimont, H. (1968) "Yield Strength and Transformation Substructure of Low-Carbon Martensite". JISI, Vol. 206, p. 325-392.

13. Nehrenberg, A. E., Payson, P. and Lillys, P. (1955) "Effect of Carbon and Nitrogen on the Attainable Hardness of Martensitic Steels". Trans. ASM, Vol. 47, p. 785-793.

14. Bain, E. C. (1939) "Functions of the Alloying Elements in Steel". American Society for Metals. p. 146-147.

15. Busby, C. C., Hawkes, M. F. and Paxton, H. W. (1955) "Tensile and Impact Properties of Low Carbon Martensites". Trans. ASM, Vol. 47, p. 135-156.

16. Cracknell, A. and Petch, N. J. (1955) "Frictional Forces on Dislocations Arrays at the Lower Yield Point in Iron". Acta Met., Vol. 3, p. 186-189.

17. Schoeck, G. and Seeger, A. (1959) "The Flow Stress of Iron and Its Dependence on Impurities". Acta Met., Vol. 7, p. 469-477.

18. Fleischer, R. L. (1962) "Solution Hardening by Tetragonal Distortions: Application to Irradiation Hardening in F.C.C. Crystals". Acta Met., Vol. 10, p. 835-842.

19. Owen, W. S., Wilson, E. A. and Bell, T. (1965) "High Strength Materials". Wiley, p. 167.

20. Roberts, M. J. and Owen, W. S. (1965) "Physical Properties of Martensite and Bainite". ISI Spec. Rpt. 93, p. 171-178.

21. Aborn, R. H. (1956) "Low Carbon Martensites." Trans. ASM, Vol. 48, p. 51-85.

22. Ansell, G. S. and Brienen, E. M. (1965) "Quench Rate Effect on the Strength of Ferrous Martensite". Trans. ASM, Vol. 58, p. 110-113.

23. Kelly, P. M. and Nutting, J. (1960) "The Martensite Transformation in Carbon Steels". Proc. Roy. Soc. of London, Vol. 259A, p. 45-58.

24. Winchell, P. G. and Cohen, M. (1963) "Solid-Solution Strengthening of Martensite by Carbon." Electron Microscopy and Strength of Crystals, Ed. Thomas, G. and Washburn, J., Interscience, p. 995-1005.

25. Radcliffe, J. V. and Schatz, M. (1963) "Effects of High Pressure on the Strength and Structure of Martensites". Nature, Vol. 200, p. 161-163.

26. McFarland, W. H. (1969) "Production and Properties of Martensitic Low Carbon Steel Sheets." Blast Furnace and Steel Plant, Feb., p. 132-145.

27. Muir, H., Averbach, B. L. and Cohen, M. (1955) "The Elastic Limit and Yield Behavior of Hardened Steels." Trans. ASM, Vol. 47, p. 380-399.

28. Anderson, J. B. R. and Fitzwilson, C. H. (1968) "Low Carbon Martensite Steels for Cold Forging." Blast Furnace and Steel Plant, June, p. 495-499.

29. Templin, R. L. (1948) "The Preparation of Test Specimens". ASM Metals Handbook. ASM, Figure 2, p. 87.

30. Dieter, G. E. (1961) "Mechanical Metallurgy". McGraw-Hill, p. 123.

31. Grange, R. A. and Stewart, H. M. (1946) "The Temperature Range of Martensite Formation". Trans., AIMME, Vol. 167, p. 484.

32. Kehl, G. L. (1949). "The Principles of Metallographic Laboratory Practice." McGraw-Hill, p. 466-470.

VITA

Allen Lewis Affolter was born August 19, 1940, at Newburg, Missouri. After graduation from Rolla High School, he entered the Missouri School of Mines in 1958 and graduated in 1962 with the degree of Bachelor of Science in Metallurgical Engineering.

He worked as a metallurgist for Inland Steel Company in East Chicago, Indiana, from 1962 until he entered the United States Army in 1963. After his release from active duty in 1968 he returned to Inland Steel Company. He entered the University of Missouri at Rolla as a graduate student in 1969.